

Compton Polarimetry @ Bonn

Wolfgang Hillert

ELectron Stretcher Accelerator

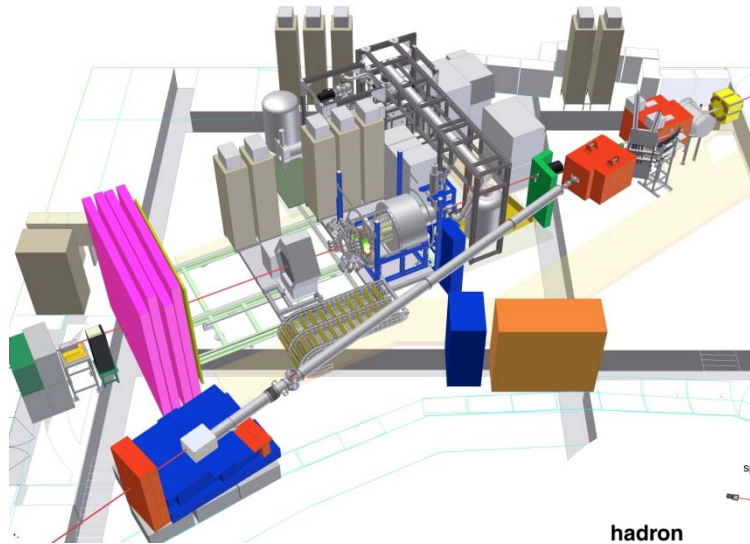


Physics Institute of Bonn University

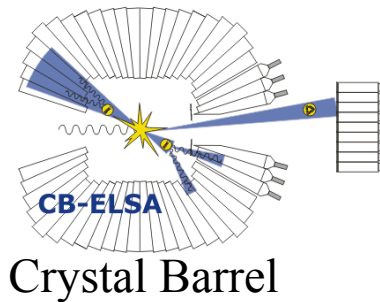
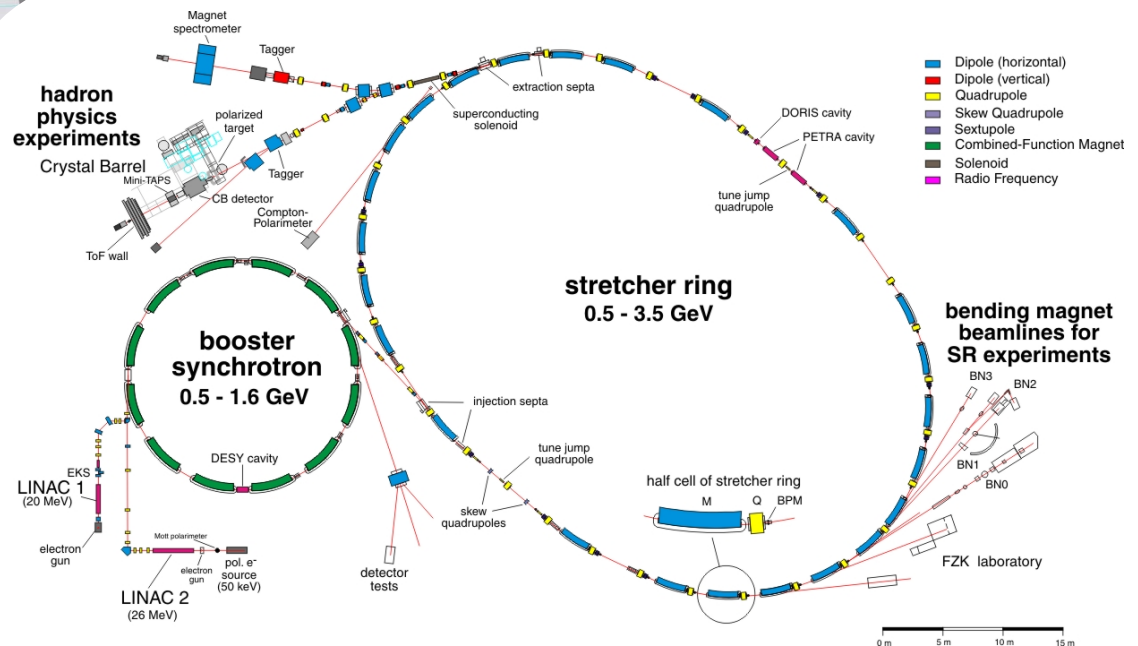
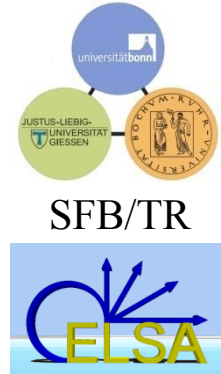
-
- Why?** → Polarised electrons @ ELSA: status and remaining problems
 - How?** → Cpol @ ELSA: Numerical simulations and design criteria
 - Past** → Ar⁺ set-up: laser control, strip detector and first measurements
 - Future** → 2-beam set-up and other improvements: expectations

Why?

Double Polarisation Experiments



external
fixed target experiments
with
**linearly and circularly
polarised photons**



BoFroST

Source of polarised electrons @ ELSA



Main features:

- inverted structure
- adjustable perveance
- load-lock-system
- pulsed 200 mJ Ti:Sa laser

Main parameters:

Beam energy:	48 keV
Pulse current:	100 mA
Repetition rate:	50 Hz
Polarisation:	≈80%
Quantum-lifetime:	>3000 h
Cathode:	Be-InGaAs/AlGaAs

Source of polarised electrons @ ELSA



Main features:

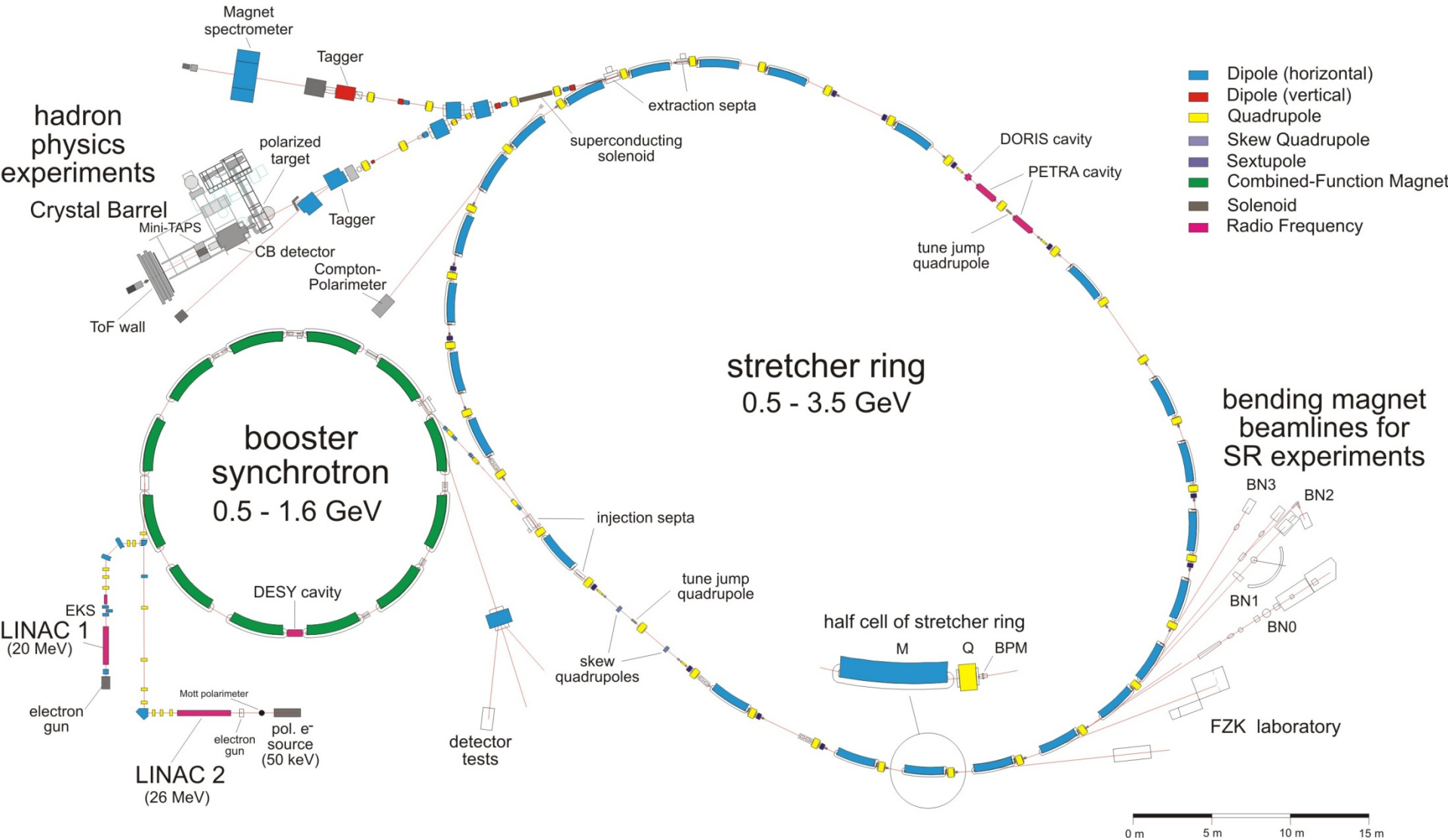
- inverted structure
- adjustable perveance
- load-lock-system
- pulsed 200 mJ Ti:Sa laser

workhorse since 2000 !!!

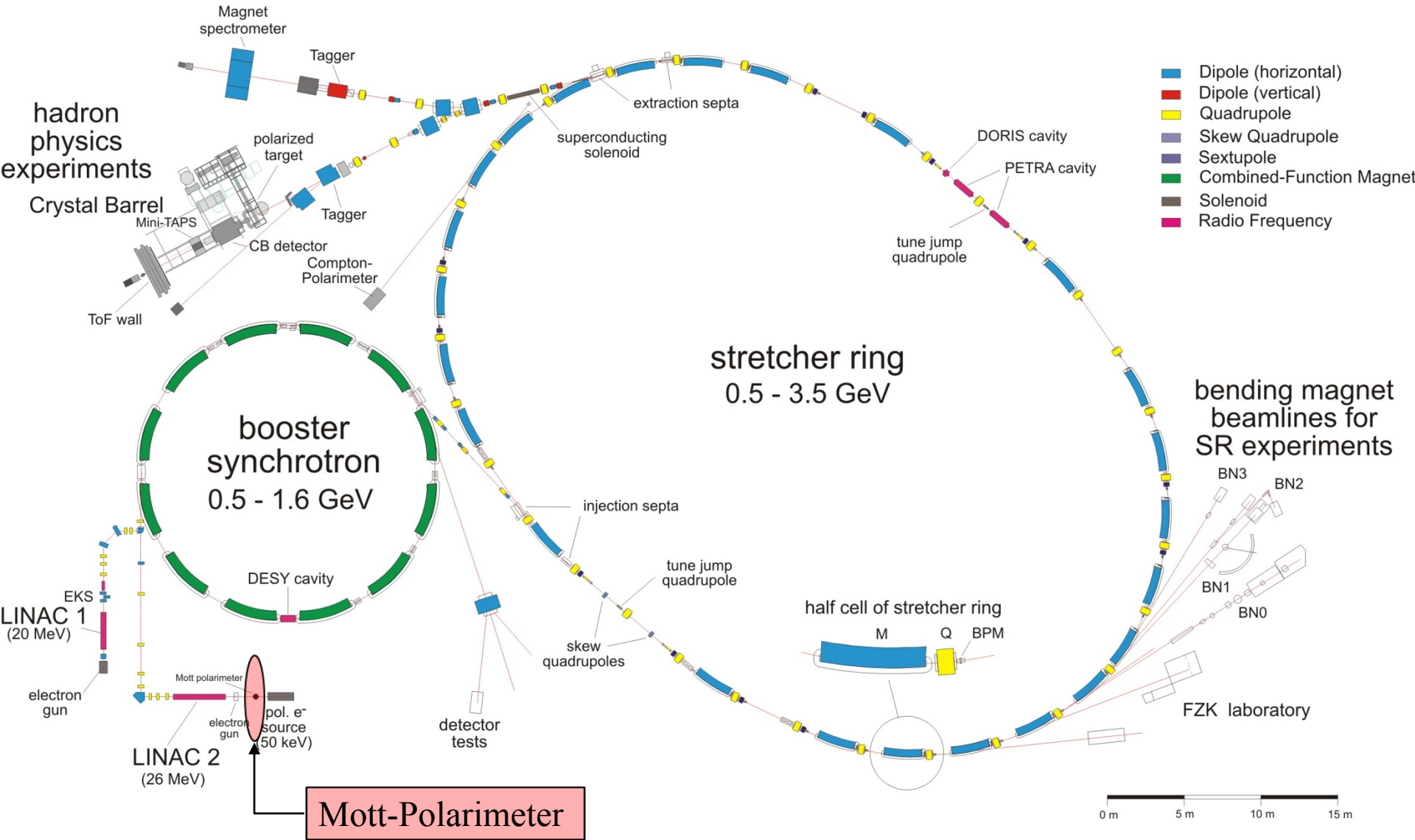
Main parameters:

Beam energy:	48 keV
Pulse current:	100 mA
Repetition rate:	50 Hz
Polarisation:	≈80%
Quantum-lifetime:	>3000 h
Cathode:	Be-InGaAs/AlGaAs

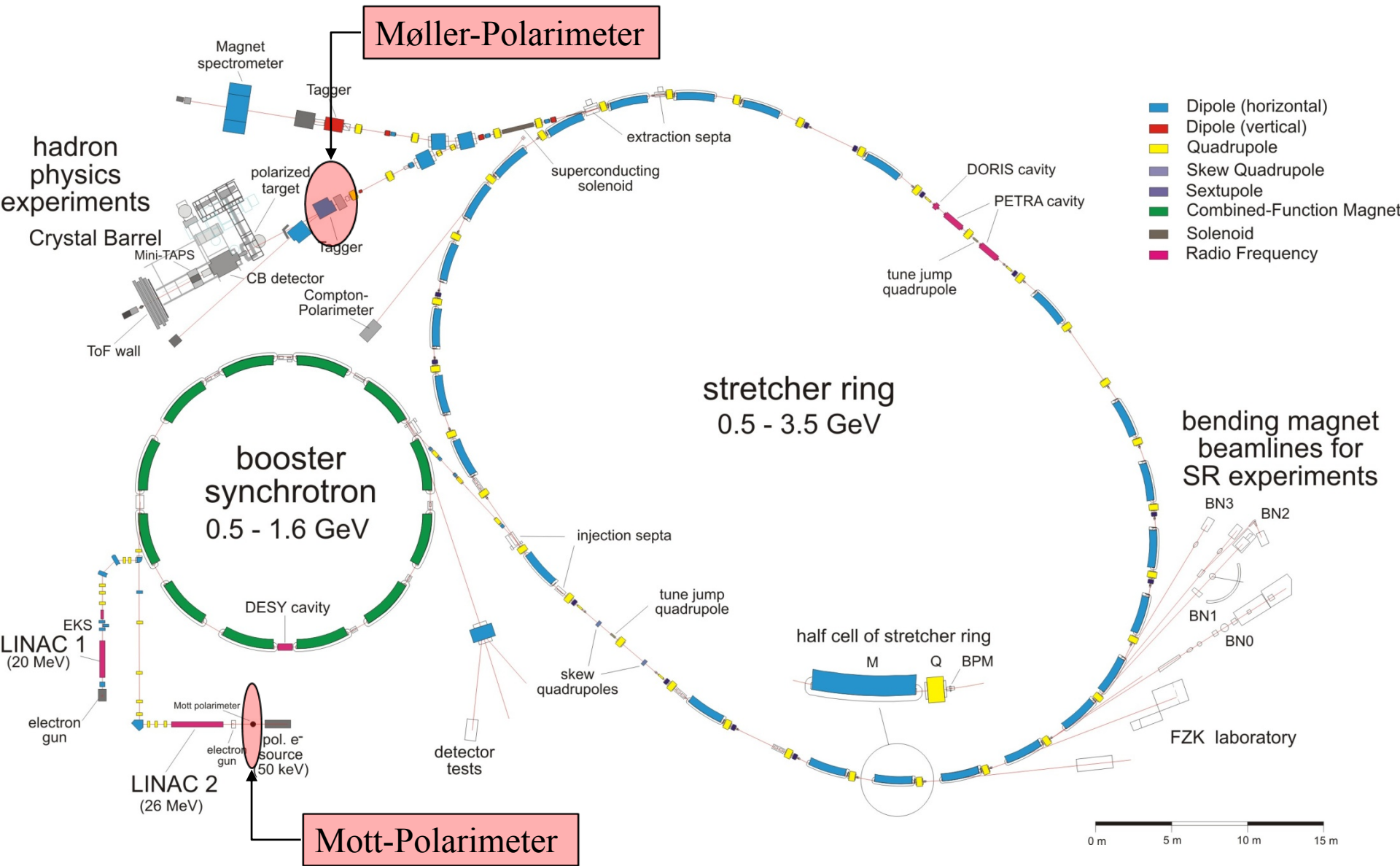
Electron Stretcher Accelerator (ELSA)



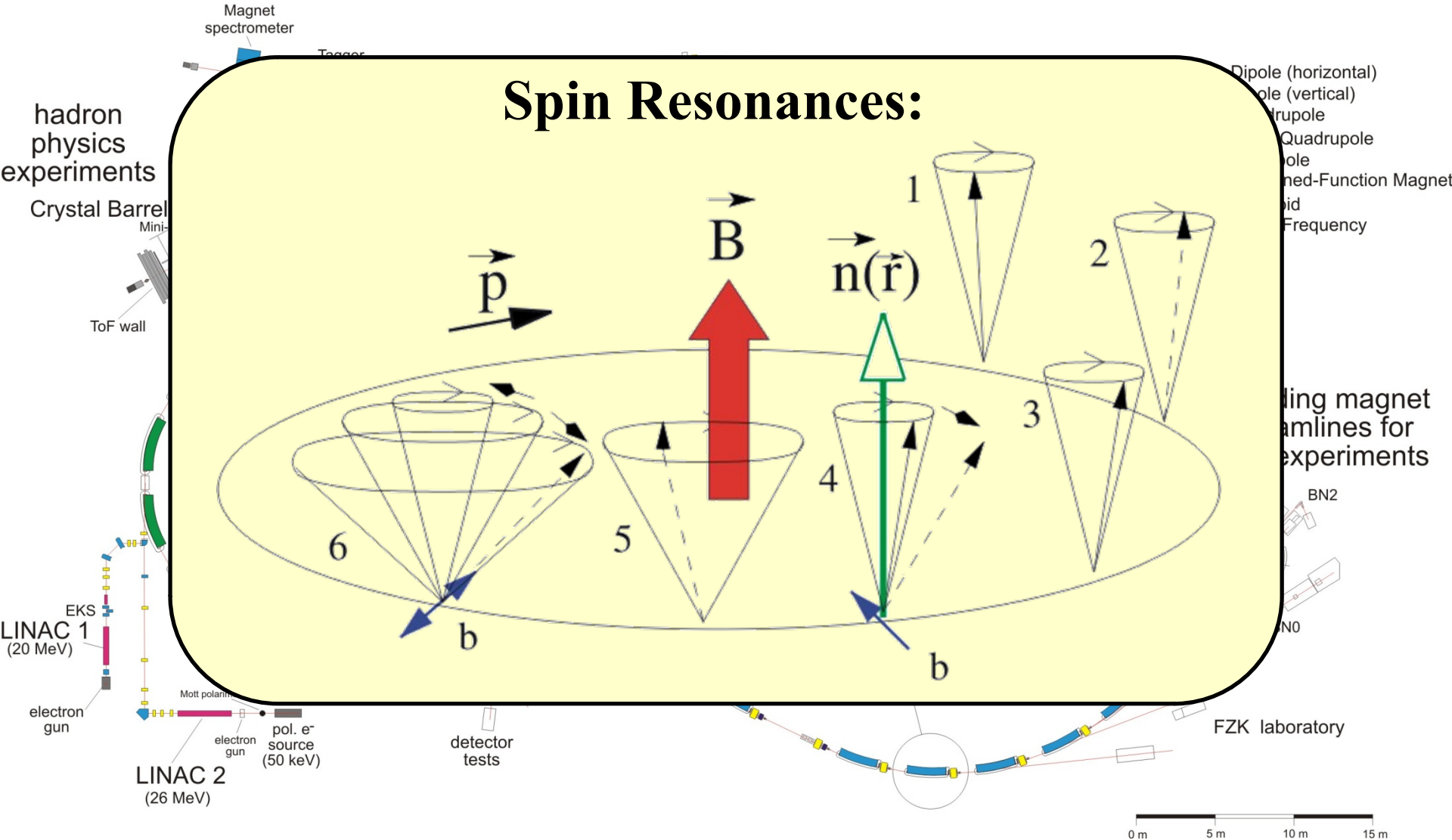
Electron Stretcher Accelerator (ELSA)



Electron Stretcher Accelerator (ELSA)

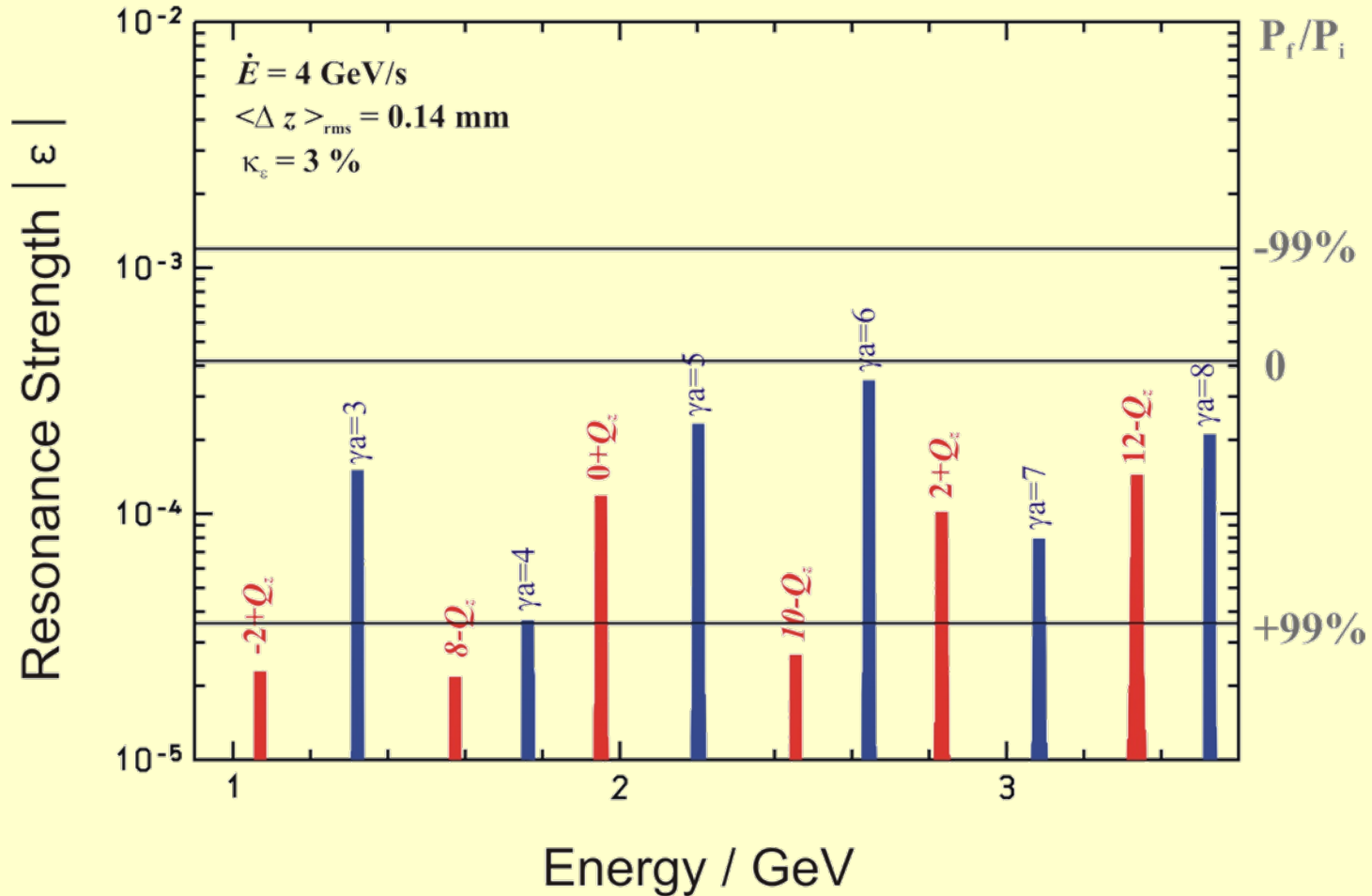


Electron Stretcher Accelerator (ELSA)



Electron Stretcher Accelerator (ELSA)

Depolarising Resonances @ ELSA



hadron
physic
experim
Crystal

ToF

EKS
LINAC 1
(20 MeV)

electron
gun

(ntal)

ole

ction Magnet

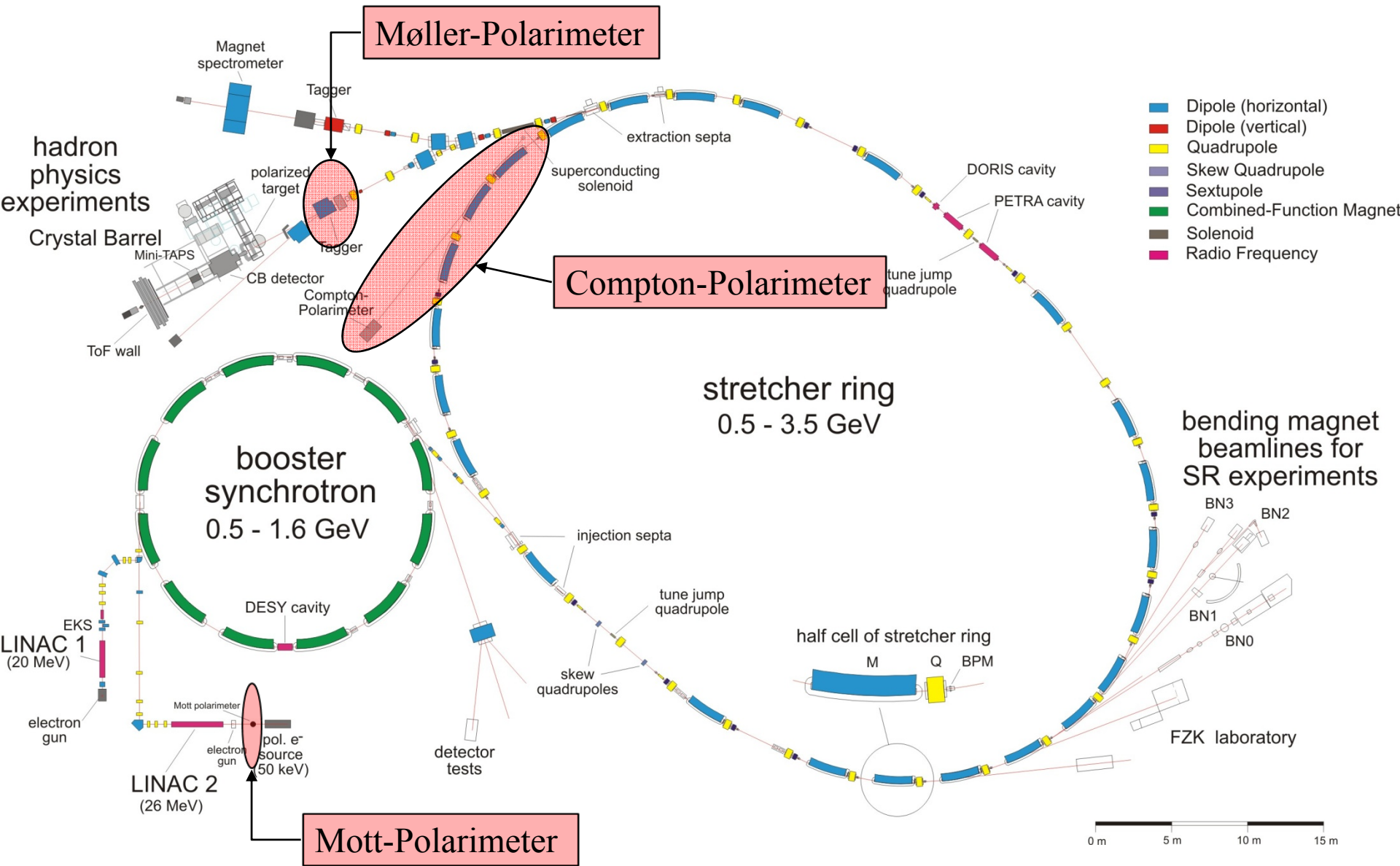
cy

magnet
es for
ments

(26

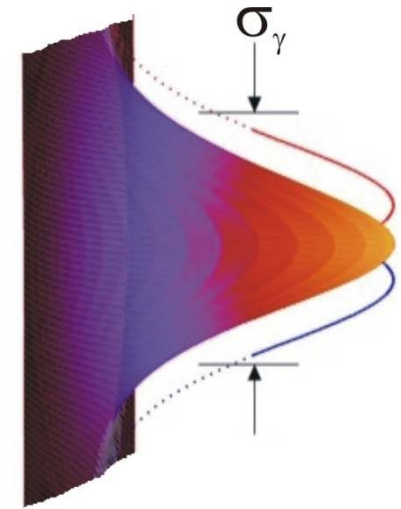
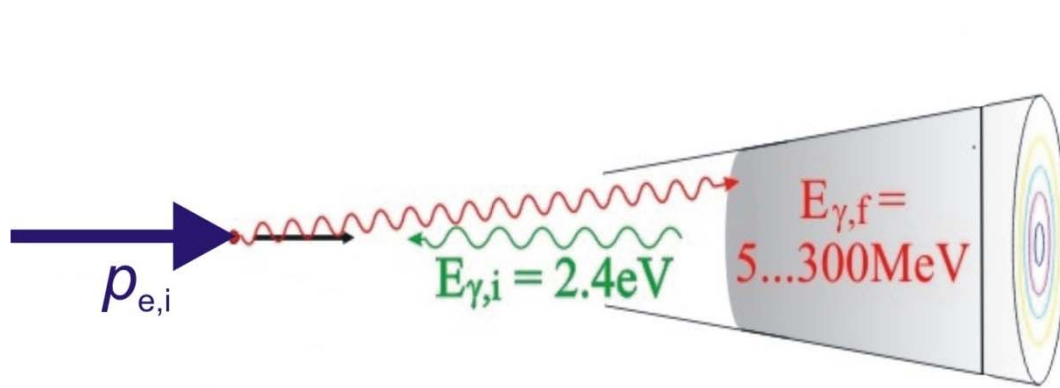
0 m 5 m 10 m 15 m

Electron Stretcher Accelerator (ELSA)



How?

Compton Scattering



Differential cross section:

$$\frac{d\sigma}{d\Omega^*}(\vec{S}, \vec{P}) = \Sigma_0 + \Sigma_1(S_1) + \Sigma_2(S_3, \vec{P})$$

Compton kinematics:

$$K_f^* = \frac{K_i^*}{1 + K_i^* \cdot (1 - \cos \vartheta^*)}$$

Polarised electrons:

$$\Sigma_2(S_3, \vec{P}) = -\underbrace{S_3 P_z \cdot CK_f^* \sin \vartheta^* (1 - \cos \vartheta^*) \sin \varphi^*}_{\Sigma_{2Z}} - \underbrace{S_3 P_s \cdot CK_f^* (1 - \cos \vartheta^*) (K_f^* + K_i^*) \cos \vartheta^*}_{\Sigma_{2S}}$$

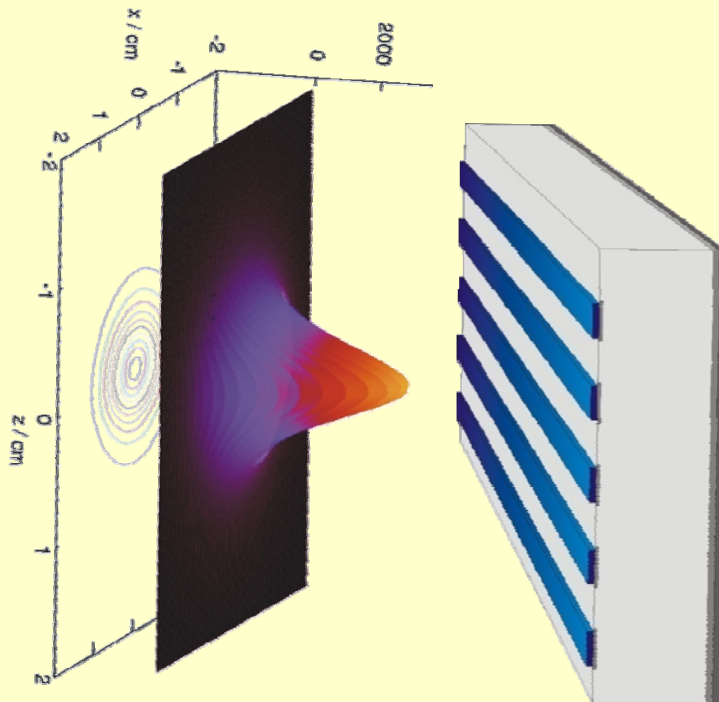
$$C = \frac{r_e^2}{2} \cdot \left(\frac{K_f^*}{K_i^*} \right)^2$$

spatial asymmetry

counting rate asymmetry

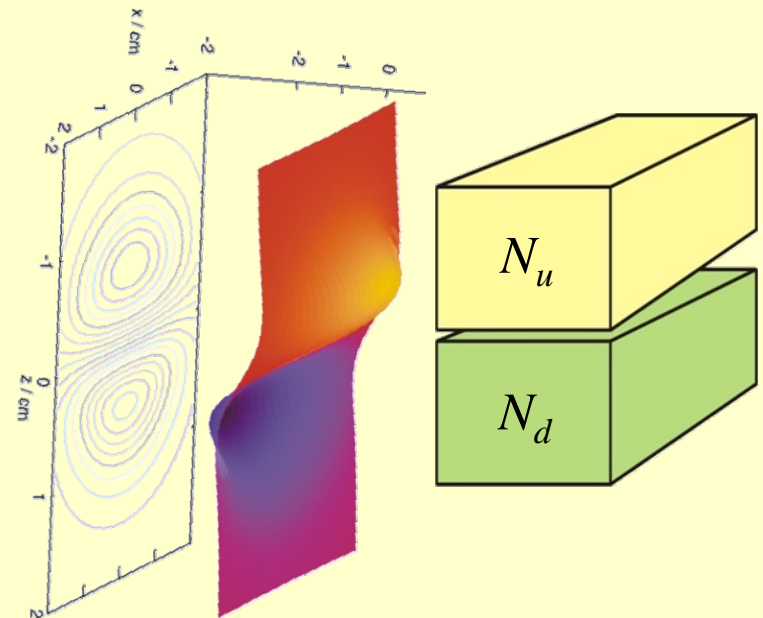
Measuring Principle

shift of the center of the
photon spatial distribution



silicon strip detector and
pair conversion required:
rather complicated

integral up-down
counting rate asymmetry

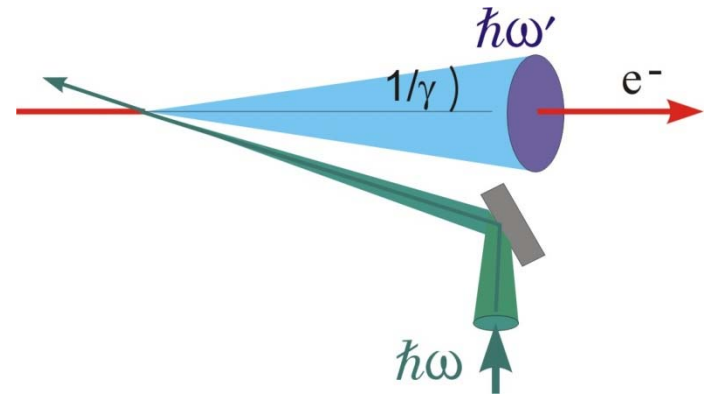


at least 2 crystal detectors and
no conversion required:
rather simple

Design Criteria

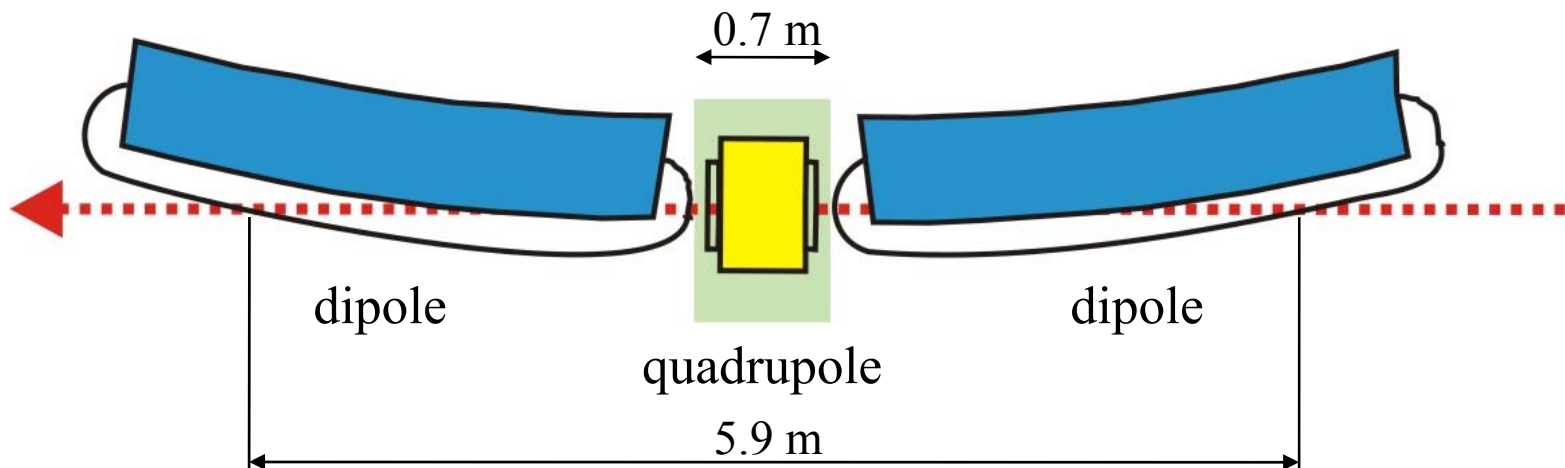
Basic Parameters:

- crossing angle: $\delta \approx 3 \text{ mrad}$
- electron beam width: $\sigma \approx 1 \text{ mm}$
- interaction region: $l \approx 0.7 \text{ m}$

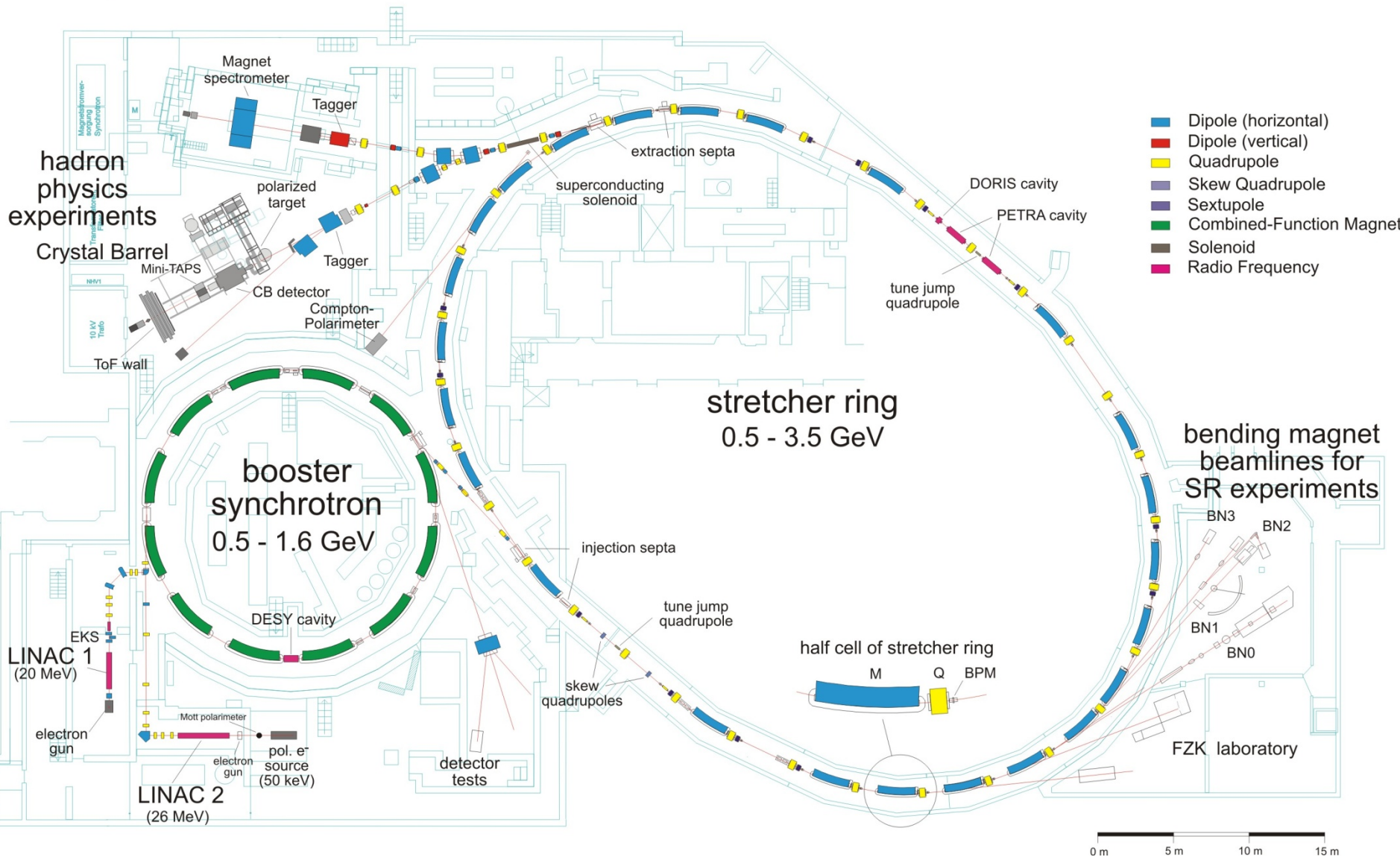


Background due to Beam-Gas Radiation:

- straight section should be considerably short!



Electron Stretcher Accelerator (ELSA)



Numerical Simulations

1. Ideal beams ($\sigma_x = \sigma_z = 0$) and infinite detector (simple):

- integral asymmetry:

$$A_{\text{int}} = \frac{\sqrt{N_u^+ N_d^-} - \sqrt{N_u^- N_d^+}}{\sqrt{N_u^+ N_d^-} + \sqrt{N_u^- N_d^+}} = \frac{\int_0^{2\pi} d\varphi^* \int_0^\pi \sin \vartheta^* d\vartheta^* \cdot \Sigma_{2Z}}{\int_0^{2\pi} d\varphi^* \int_0^\pi \sin \vartheta^* d\vartheta^* \cdot \Sigma_0} \cdot P_\gamma \cdot P_e$$

- shift of center of spatial distribution:

$$\Delta \bar{z} = \bar{z}_+ - \bar{z}_- = \frac{\int_0^{2\pi} d\varphi^* \int_0^\pi \sin \vartheta^* d\vartheta^* \cdot z(\vartheta^*, \varphi^*) \cdot \Sigma_{2Z}}{\int_0^{2\pi} d\varphi^* \int_0^\pi \sin \vartheta^* d\vartheta^* \cdot \Sigma_0} \cdot P_\gamma \cdot P_e$$

$$\left(\text{with } z(\vartheta^*, \varphi^*) = \frac{D}{\gamma} \cdot \frac{\sin \vartheta^* (\beta - \cos \vartheta^*)}{(1 - \beta \cos \vartheta^*)^2} \cos \varphi^* \right)$$

1-dim integration:



Numerical Simulations

2. Ideal beams ($\sigma_x = \sigma_z = 0$) and finite detector (moderate):

– integral asymmetry:

$$A_{\text{int}} = \frac{\int_{-X_{\text{det}}/2}^{X_{\text{det}}/2} dx \int_0^{Z_{\text{det}}/2} dz \cdot \frac{\partial(\mathcal{G}^*, \varphi^*)}{\partial(x, z)} \cdot \Sigma_{2Z}(\mathcal{G}^*(x, z), \varphi^*(x, z))}{\int_{-X_{\text{det}}/2}^{X_{\text{det}}/2} dx \int_0^{Z_{\text{det}}/2} dz \cdot \frac{\partial(\mathcal{G}^*, \varphi^*)}{\partial(x, z)} \cdot \Sigma_0(\mathcal{G}^*(x, z), \varphi^*(x, z))} \cdot P_\gamma \cdot P_e$$

– shift of center of spatial distribution:

$$\Delta \bar{z} = \frac{\int_{-X_{\text{det}}/2}^{X_{\text{det}}/2} dx \int_{-Z_{\text{det}}/2}^{Z_{\text{det}}/2} dz \cdot \frac{\partial(\mathcal{G}^*, \varphi^*)}{\partial(x, z)} \cdot z \cdot \Sigma_{2Z}(\mathcal{G}^*(x, z), \varphi^*(x, z))}{\int_{-X_{\text{det}}/2}^{X_{\text{det}}/2} dx \int_0^{Z_{\text{det}}/2} dz \cdot \frac{\partial(\mathcal{G}^*, \varphi^*)}{\partial(x, z)} \cdot \Sigma_0(\mathcal{G}^*(x, z), \varphi^*(x, z))} \cdot P_\gamma \cdot P_e$$

$$\left(\text{with: } \frac{\partial(\mathcal{G}^*, \varphi^*)}{\partial(x, z)} = \left(\frac{\gamma}{D}\right)^2 \cdot \frac{(1 - \beta \cos \mathcal{G}^*)^3}{\beta - \cos \mathcal{G}^*}\right)$$

2-dim integration:

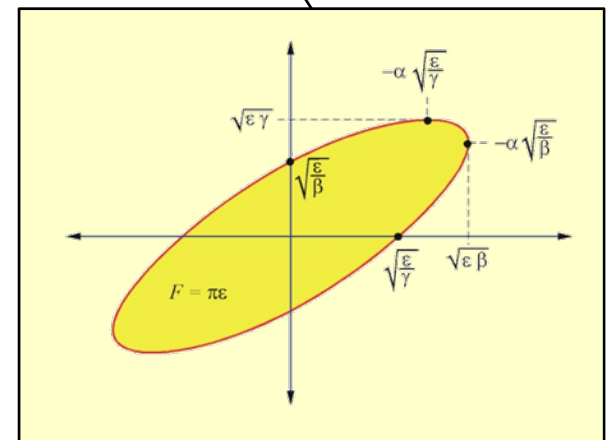
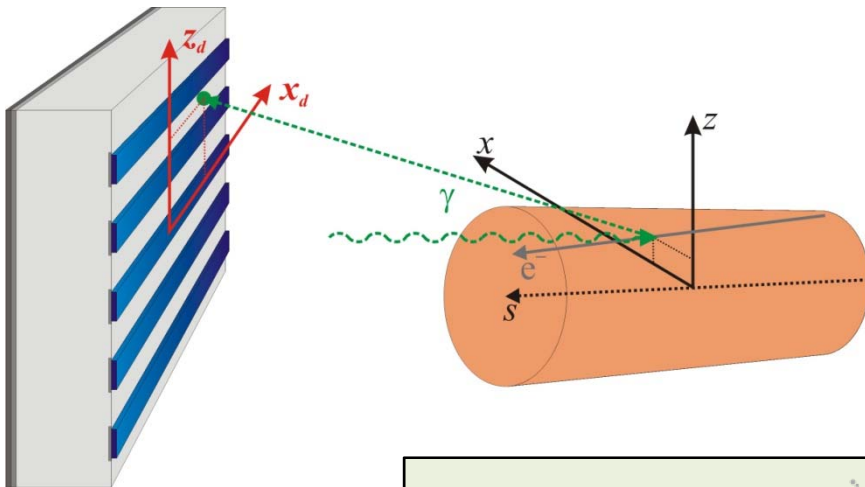


Numerical Simulations

3. Real beams ($\sigma_x, \sigma_z, \sigma_{x'}, \sigma_{z'} \neq 0$) and finite detector (!!!):

a) 2-D intensity profile of backscattered photons:

$$\dot{N}(x_d, z_d) = \int_{S_0}^{S_1} ds \int_{Z_{\min}}^{Z_{\max}} dz \int_{X_{\min}}^{X_{\max}} dx \int_{Z'_{\min}}^{Z'_{\max}} dz' \int_{X'_{\min}}^{X'_{\max}} dx' \frac{\partial(\mathcal{G}^*, \varphi^*)}{\partial(x, z)} \cdot \rho_e(s, x, z, x', z') \cdot \rho_\gamma(s, x, z) \cdot \frac{d\sigma}{d\Omega^*}$$



5-dim integration:



Numerical Simulations

3. Real beams ($\sigma_x, \sigma_z, \sigma_x', \sigma_z' \neq 0$) and finite detector (!!!):

b) Asymmetry and shift from mean values:

- integral asymmetry:

$$\left. \begin{aligned} \dot{N}_u^{+,-} &= \sum_{i,j}^{\forall z_j \geq 0} \dot{N}^{+,-}(x_i, z_j) \\ \dot{N}_d^{+,-} &= \sum_{i,j}^{\forall z_j \leq 0} \dot{N}^{+,-}(x_i, z_j) \end{aligned} \right\} A_{\text{int}} = \frac{\sqrt{\dot{N}_u^+ \dot{N}_d^-} - \sqrt{\dot{N}_u^- \dot{N}_d^+}}{\sqrt{\dot{N}_u^+ \dot{N}_d^-} + \sqrt{\dot{N}_u^- \dot{N}_d^+}}$$

- shift of center of spatial distribution:

$$\Delta \bar{z} = \sum_{i,j} z_j \dot{N}^+(x_i, z_j) - \sum_{i,j} z_j \dot{N}^-(x_i, z_j)$$

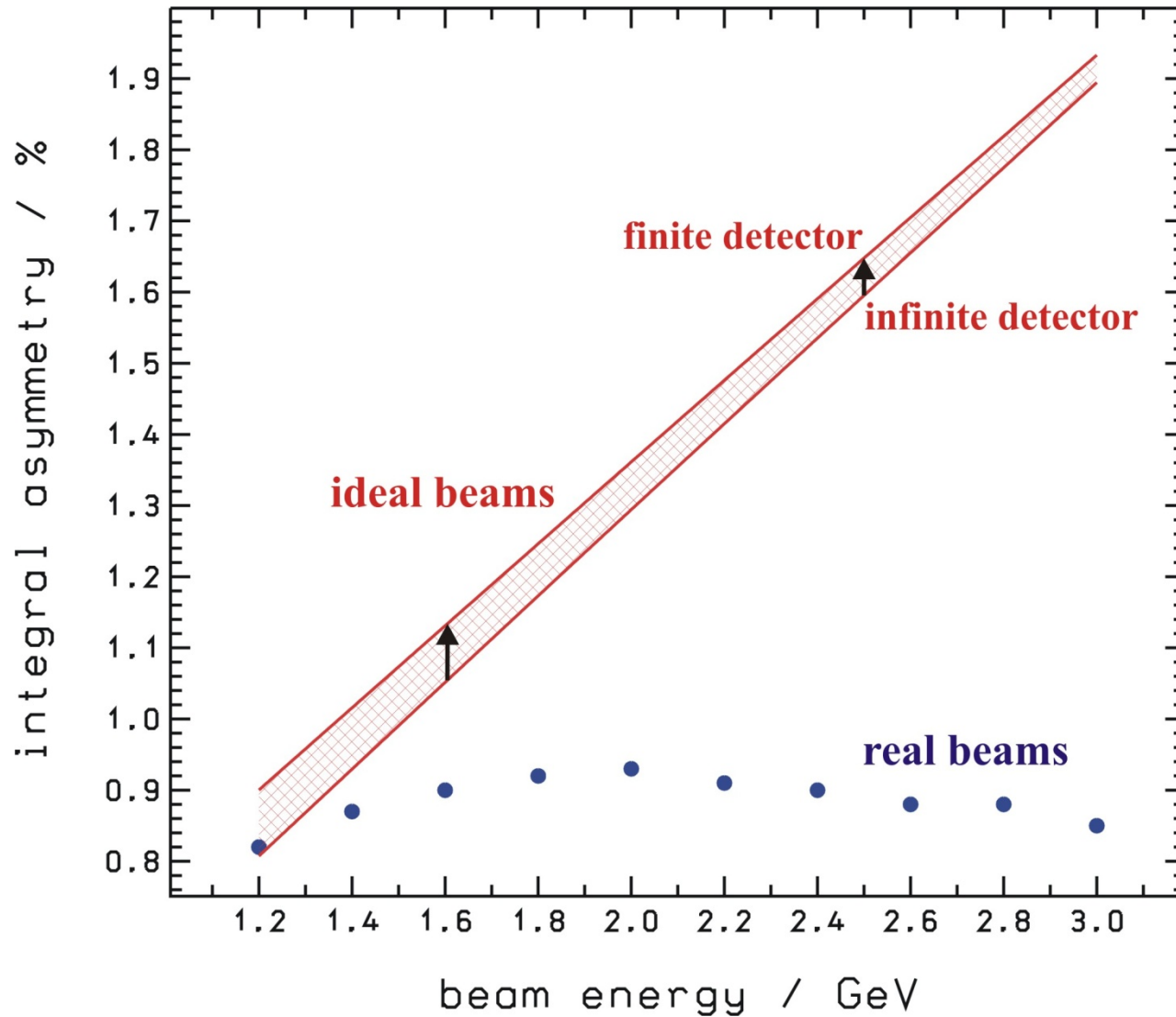
#15744 5-dim integrations:



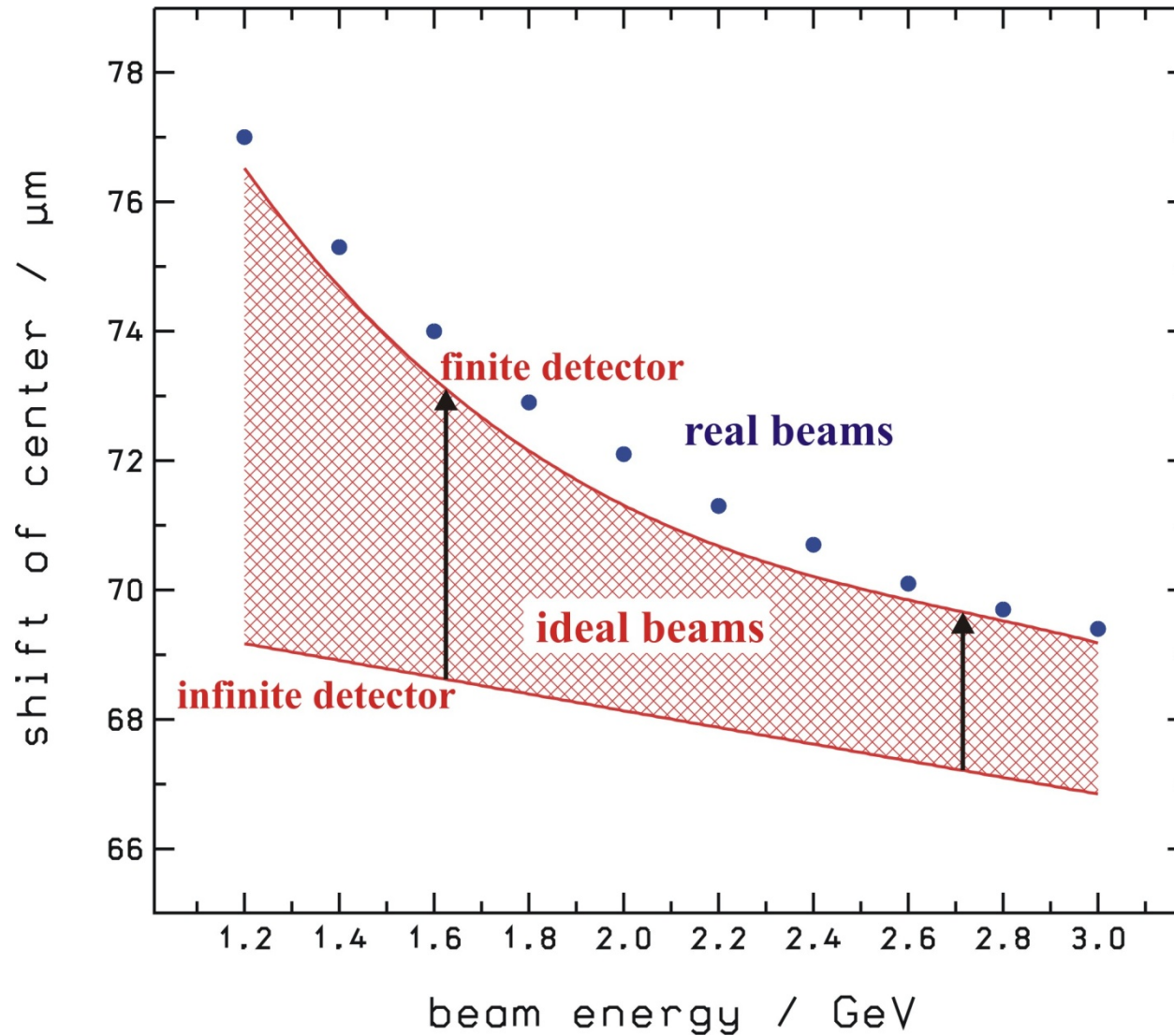
5-dim integration for each point:

- detector size = 4.0 x 3.84 cm²
- detector pitch = 100μm
- in total 41 x 384 points

Counting Rate Asymmetry

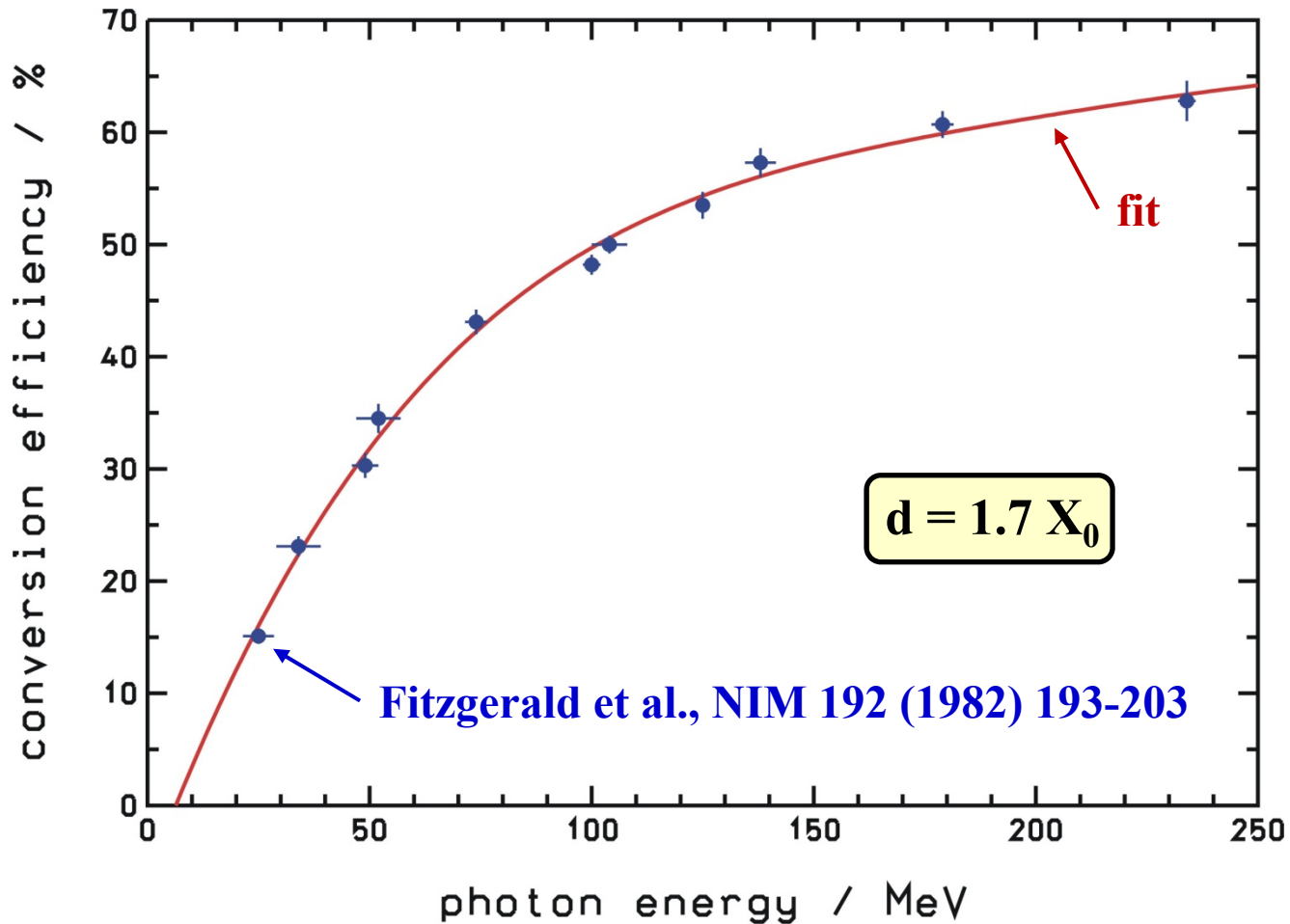


Shift of Spatial Distribution

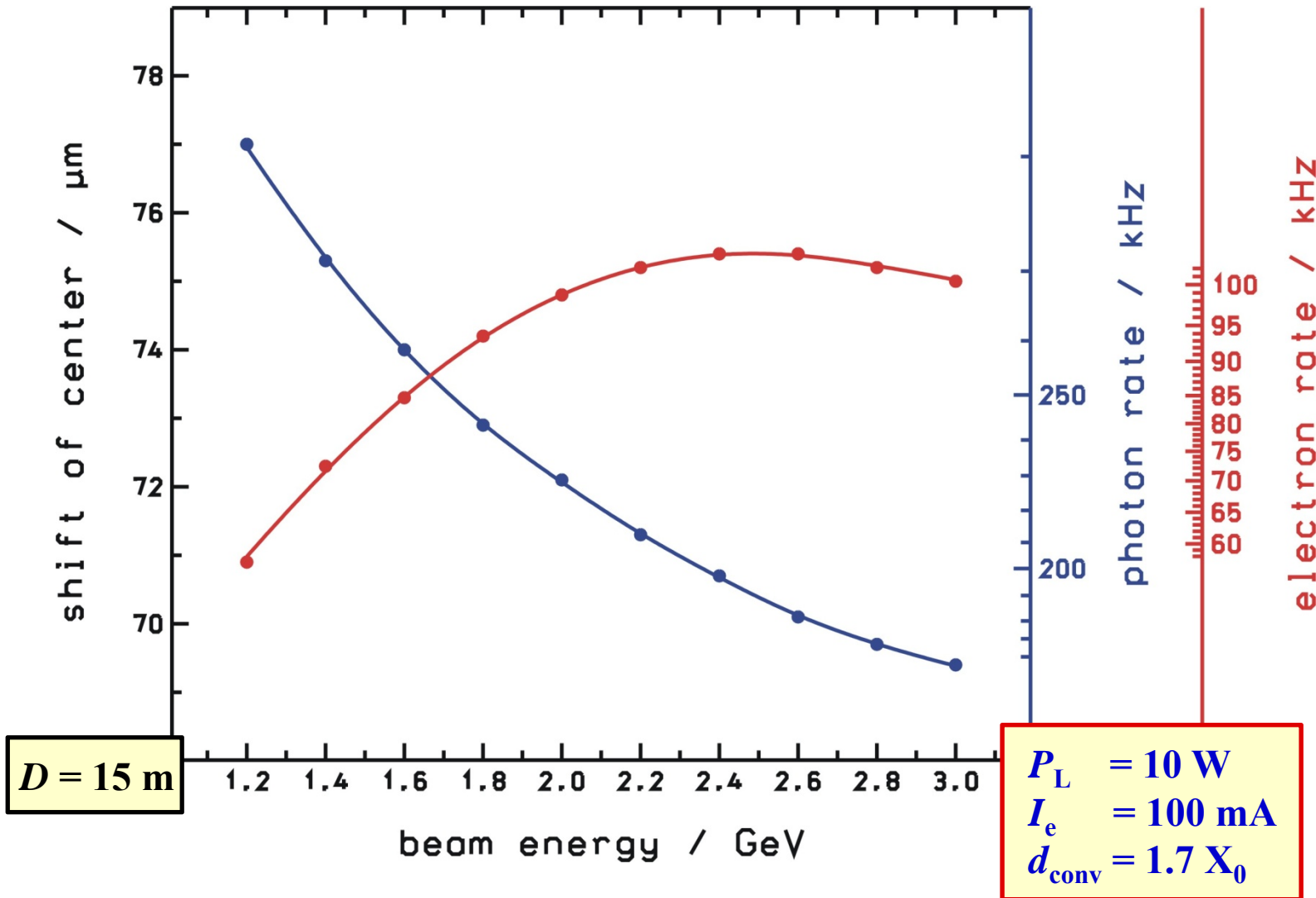


Numerical Simulations

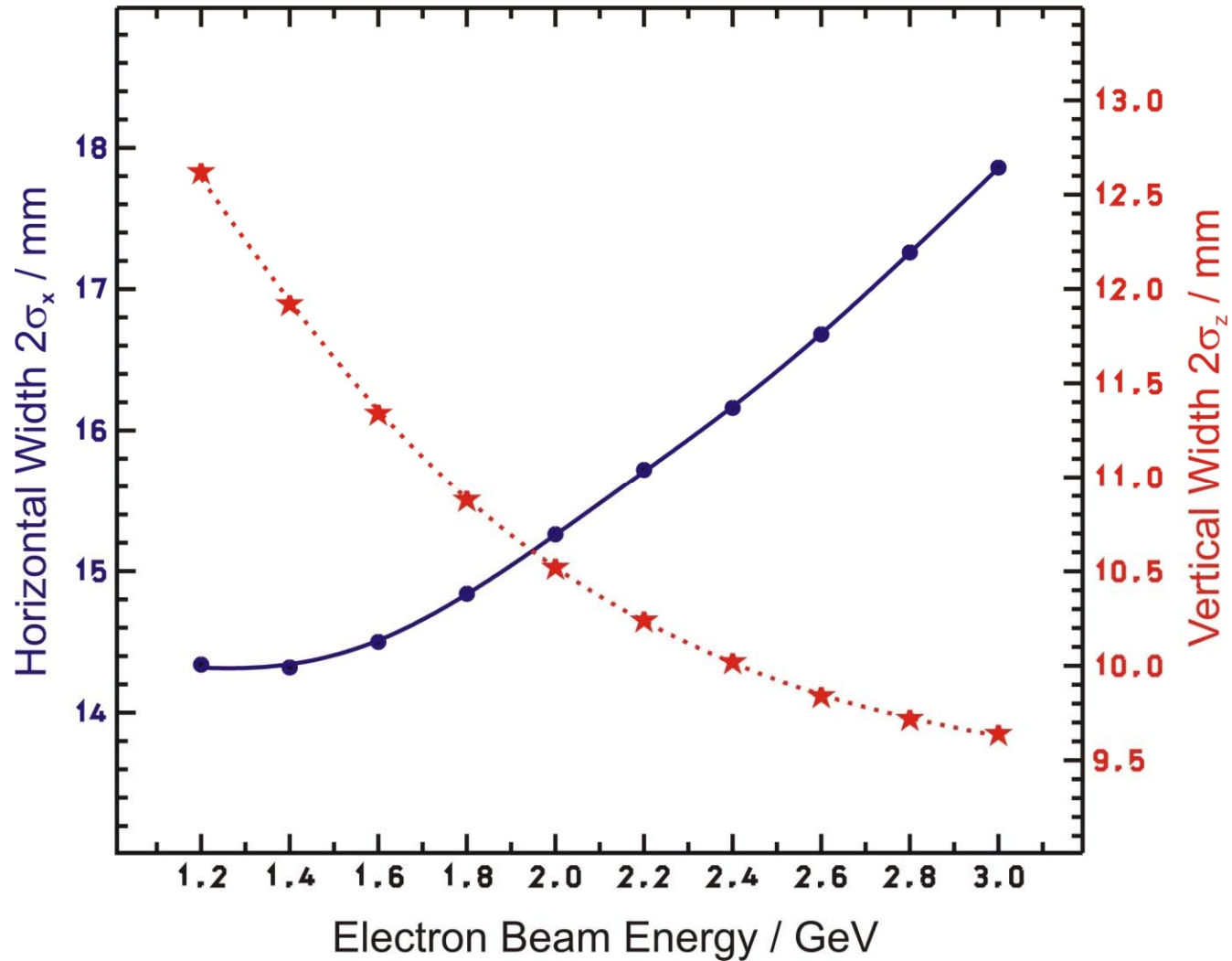
4. Pair conversion (e^+/e^-):



Analysing Power

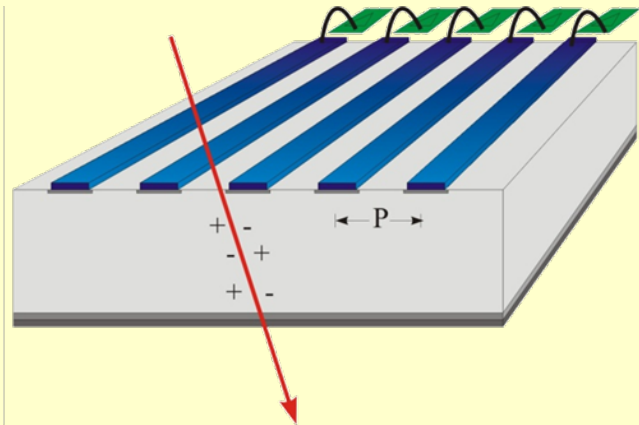


Beam Parameters



Required Pitch

Strip detector with pitch p :

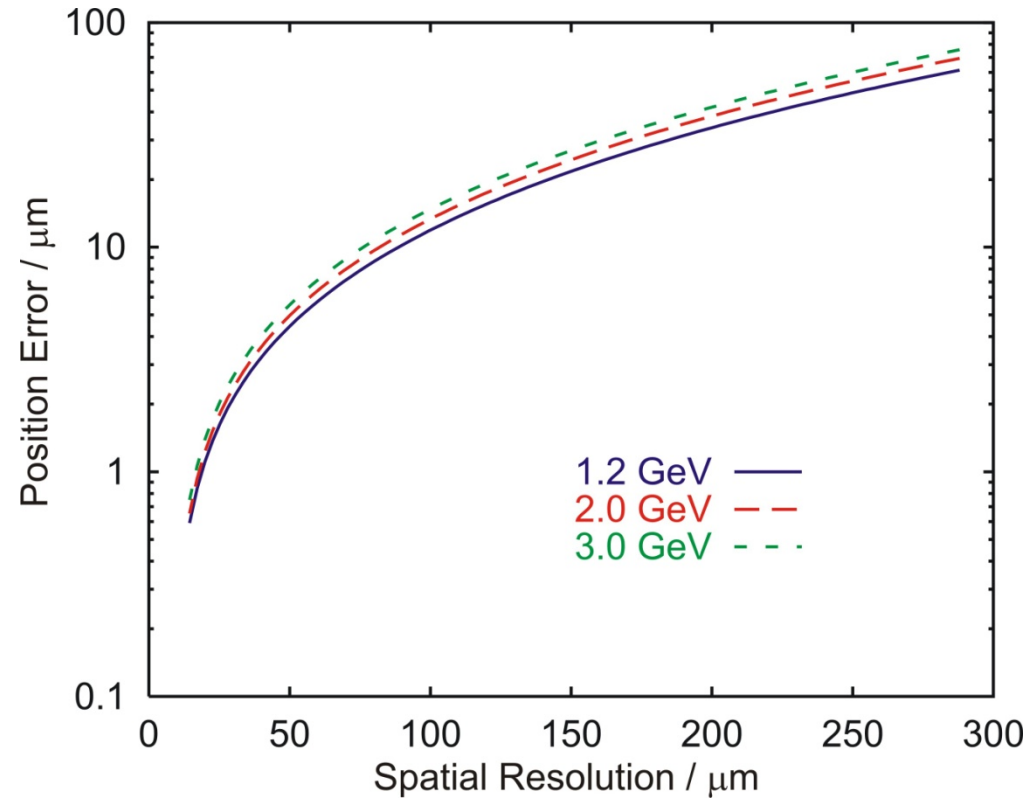


• spatial resolution:

$$\Delta z_{\text{det}} = \frac{p}{\sqrt{12}}$$

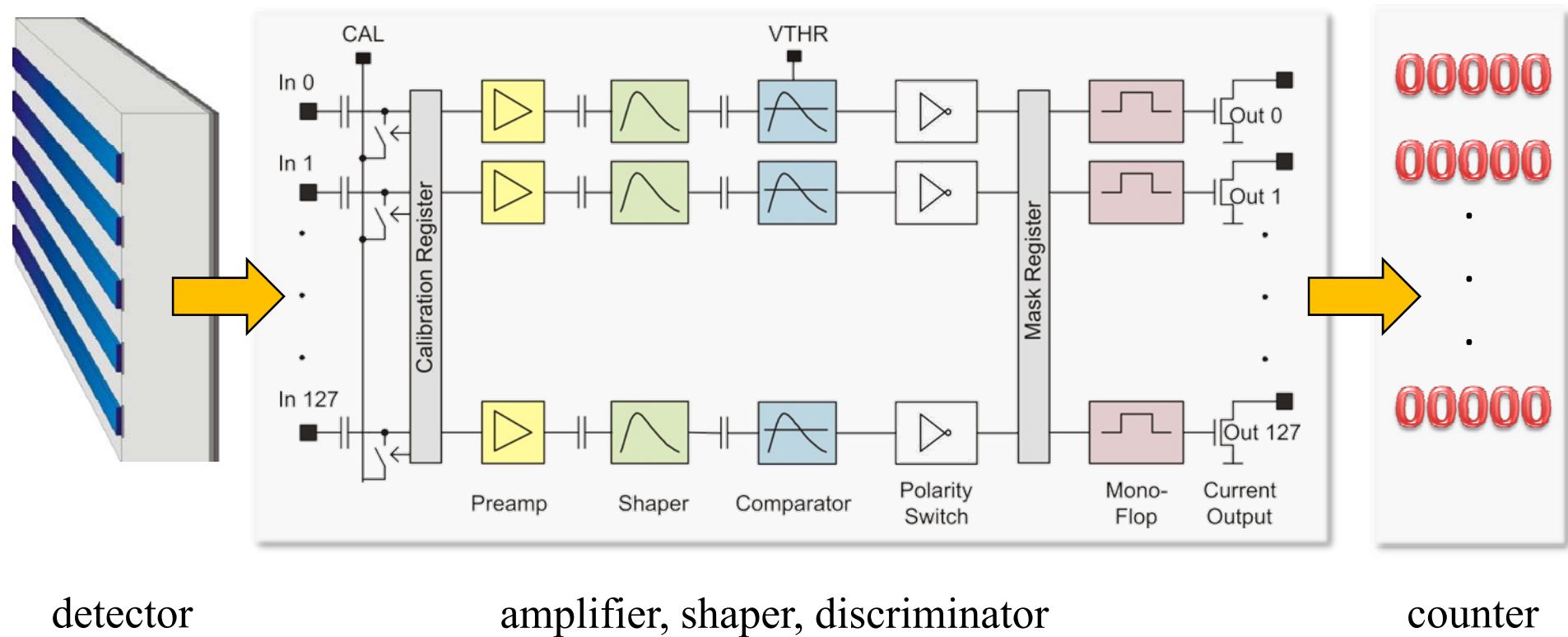
• achievable position error:

$$\Delta \bar{z} = \sqrt{\frac{\sigma_z^2}{N^2} + \frac{\sum_i n_i^2}{N^2} \cdot \Delta z_{\text{det}}^2} \xrightarrow{N \rightarrow \infty} \Delta z_{\infty}$$



$\Delta P \leq 1\% \leftrightarrow \Delta z \leq 0.7 \mu\text{m} \leftrightarrow p \approx 50 \mu\text{m}$

Counting Microstrip Detector



detector

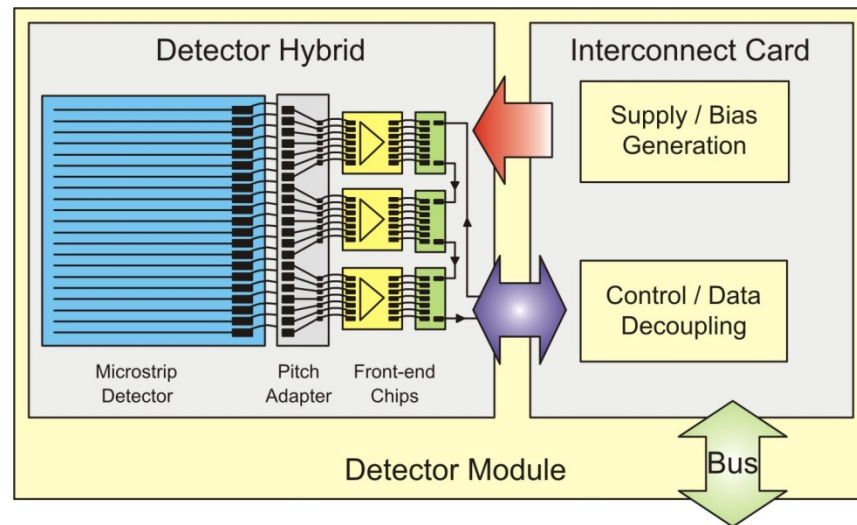
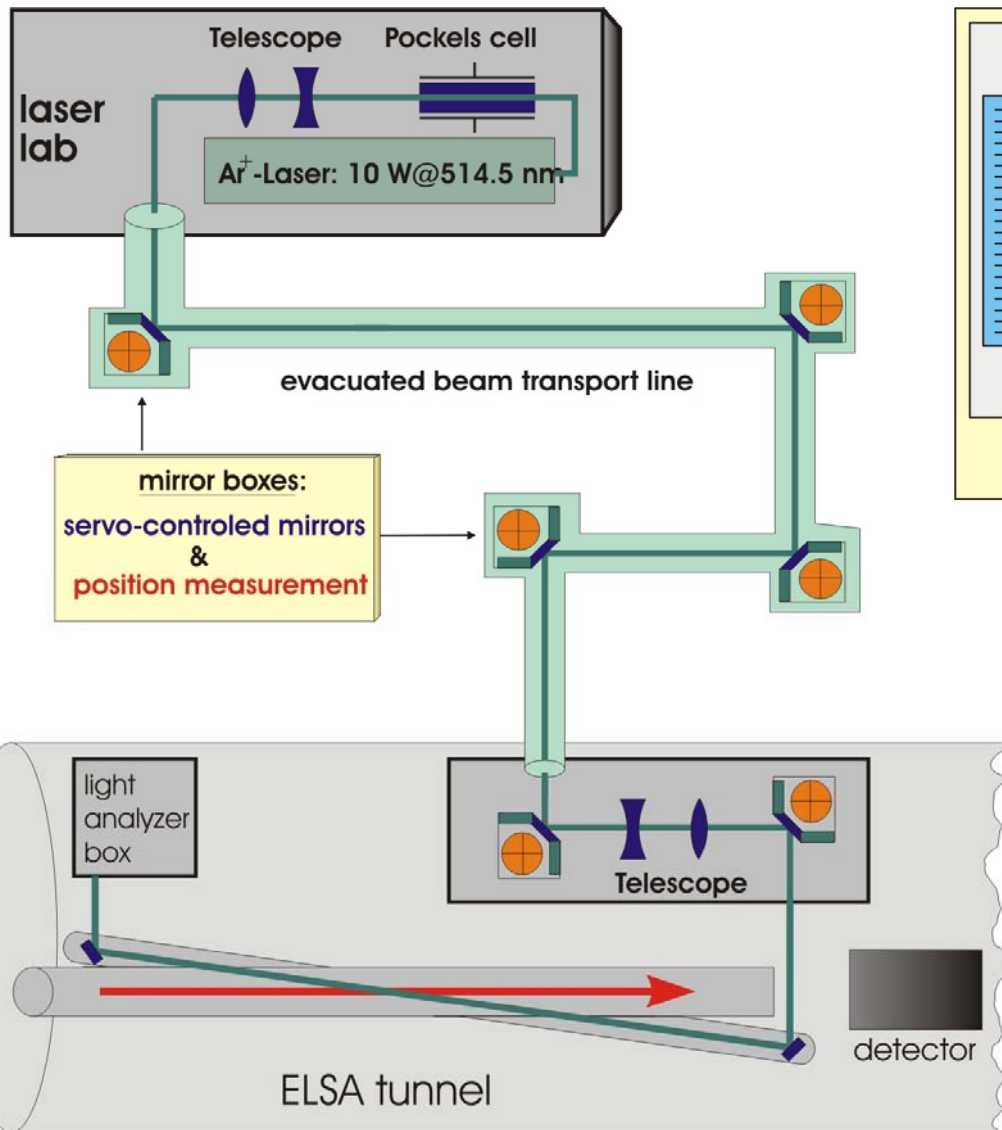
amplifier, shaper, discriminator

counter

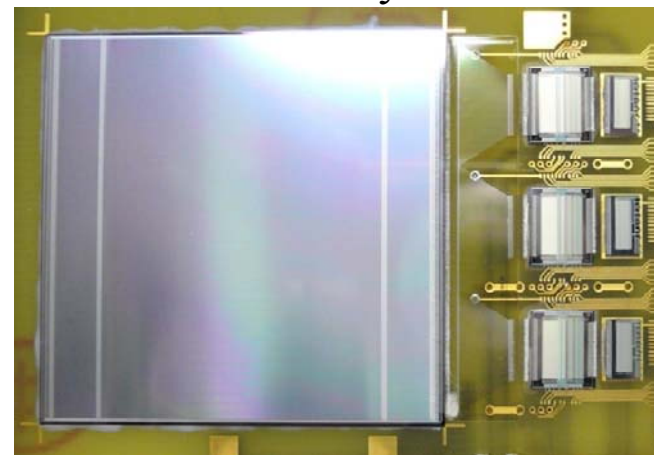
Developed in close collaboration with ATLAS pixel-detector group of N. Wermes, PI Bonn

Past

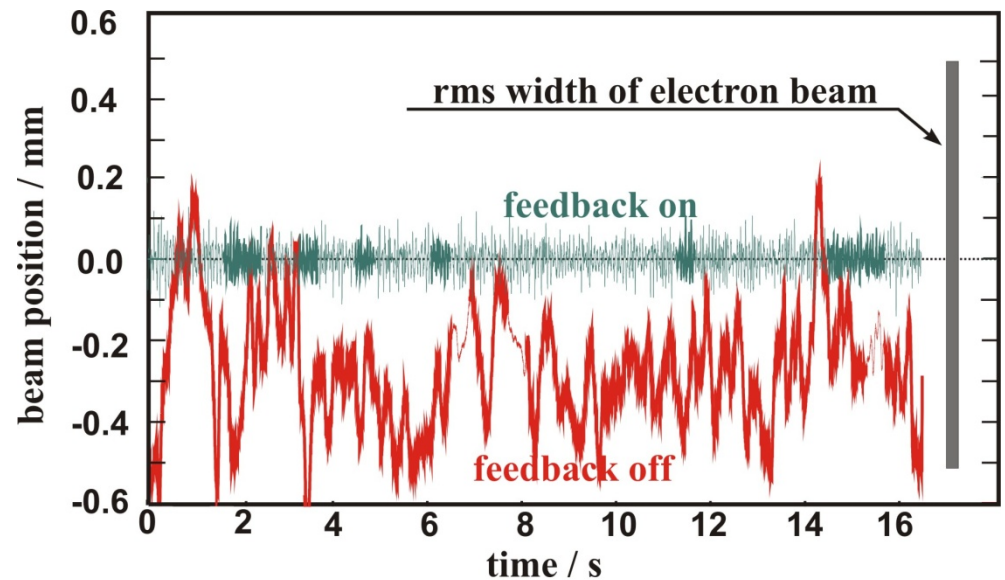
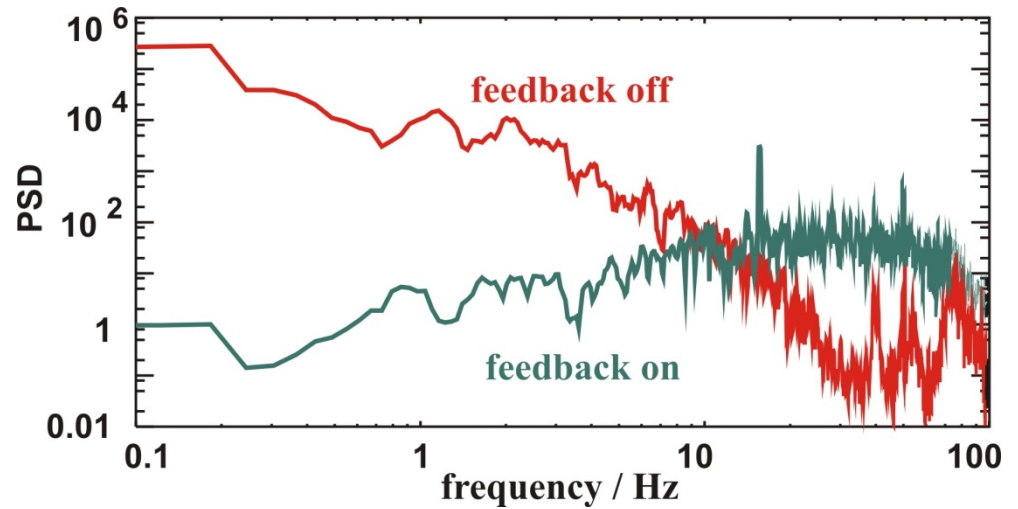
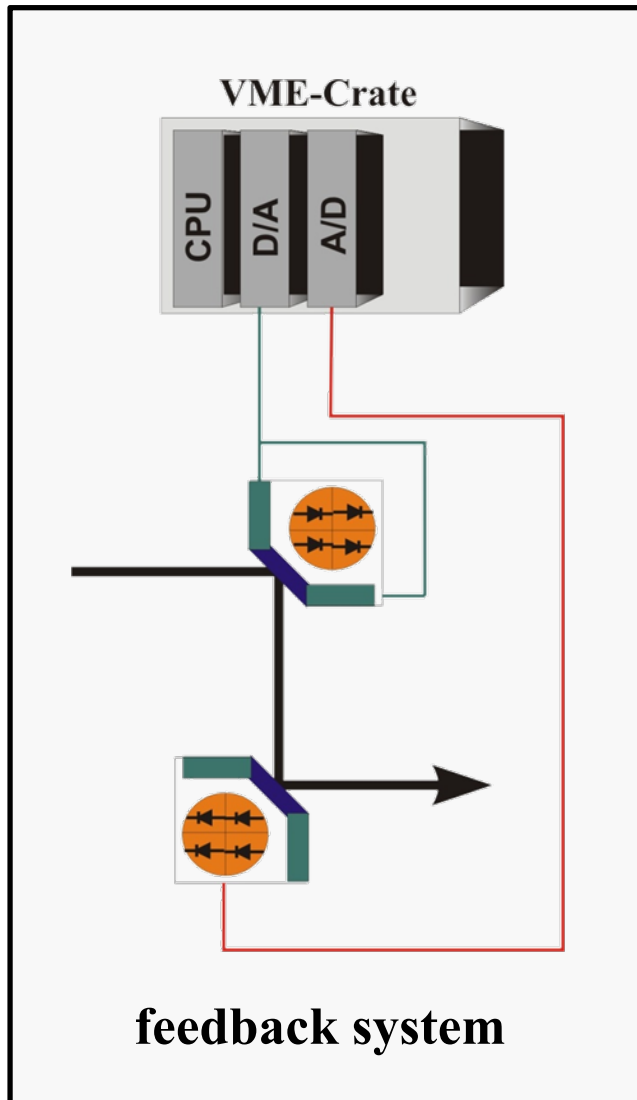
Ar⁺ Set-Up:



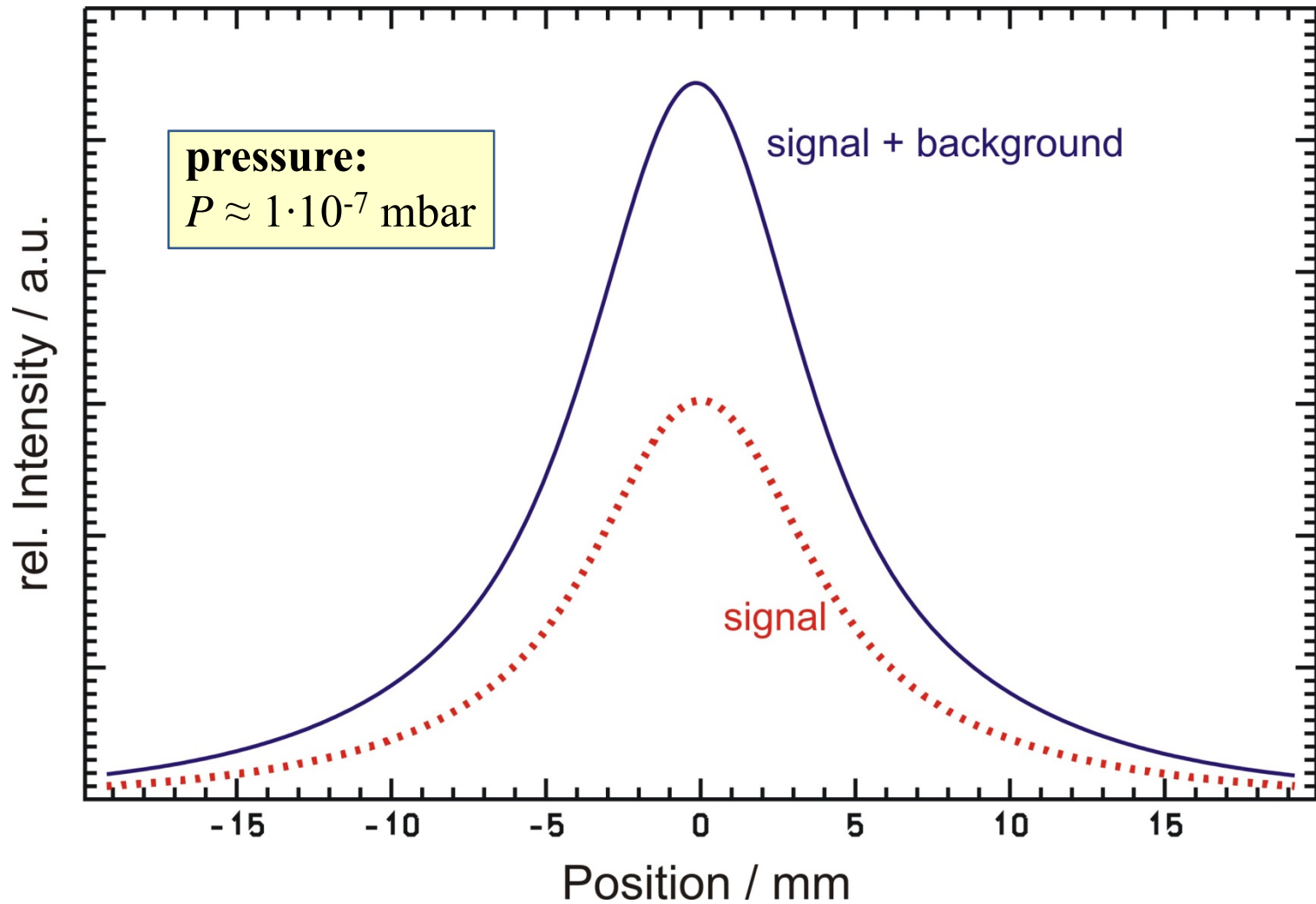
Detector Hybrid:



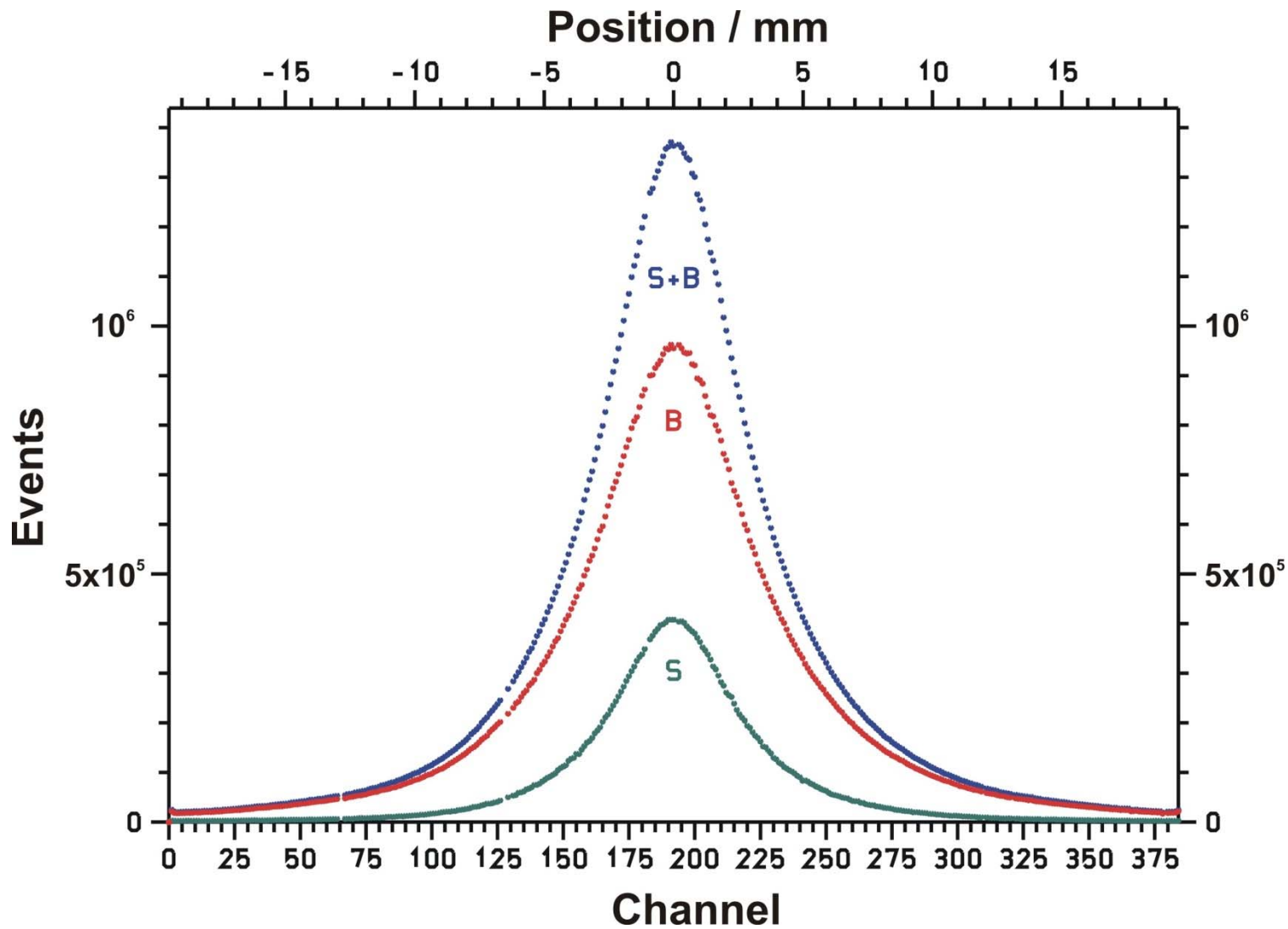
Beam Pointing Stability



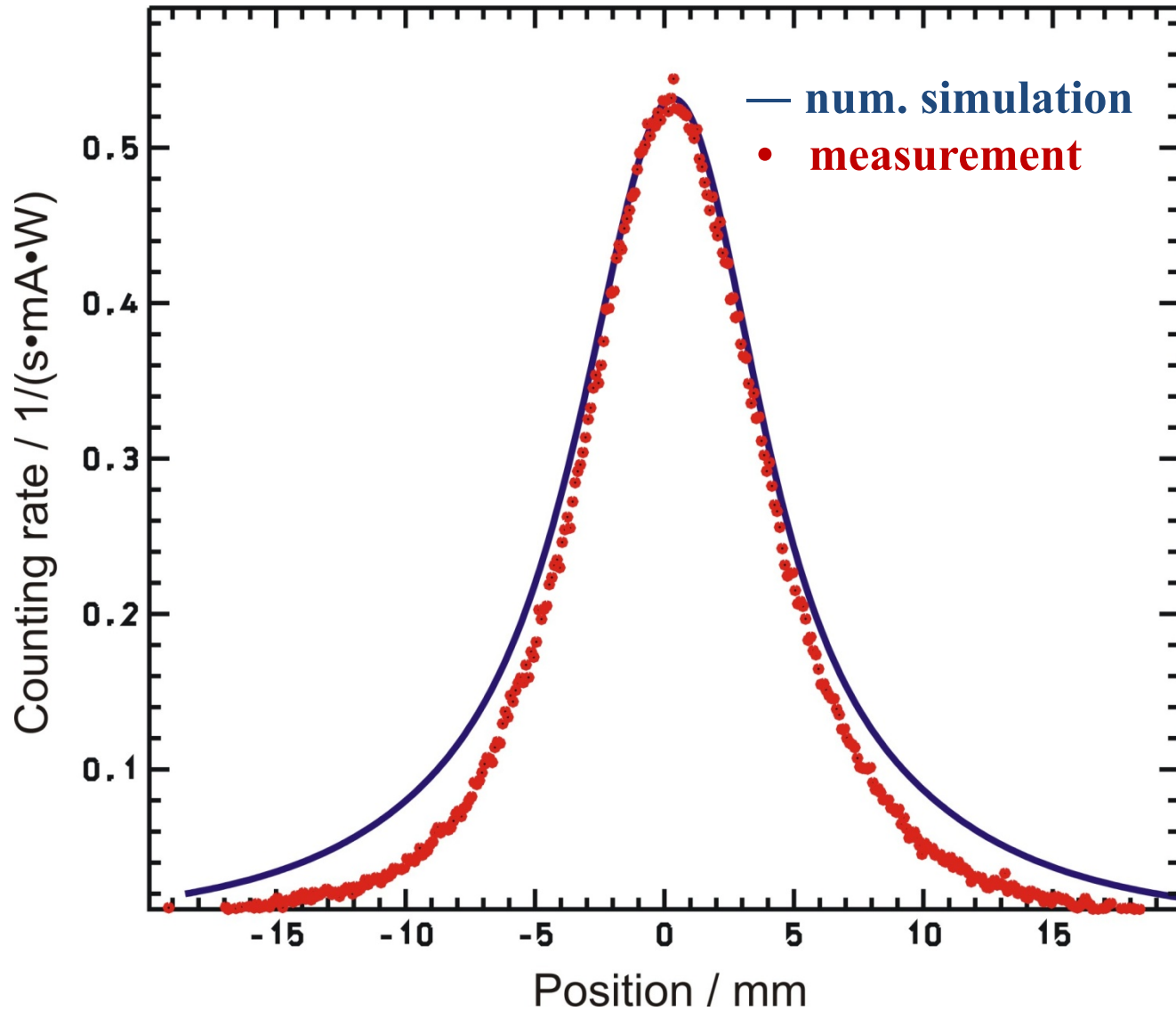
Signal / Background



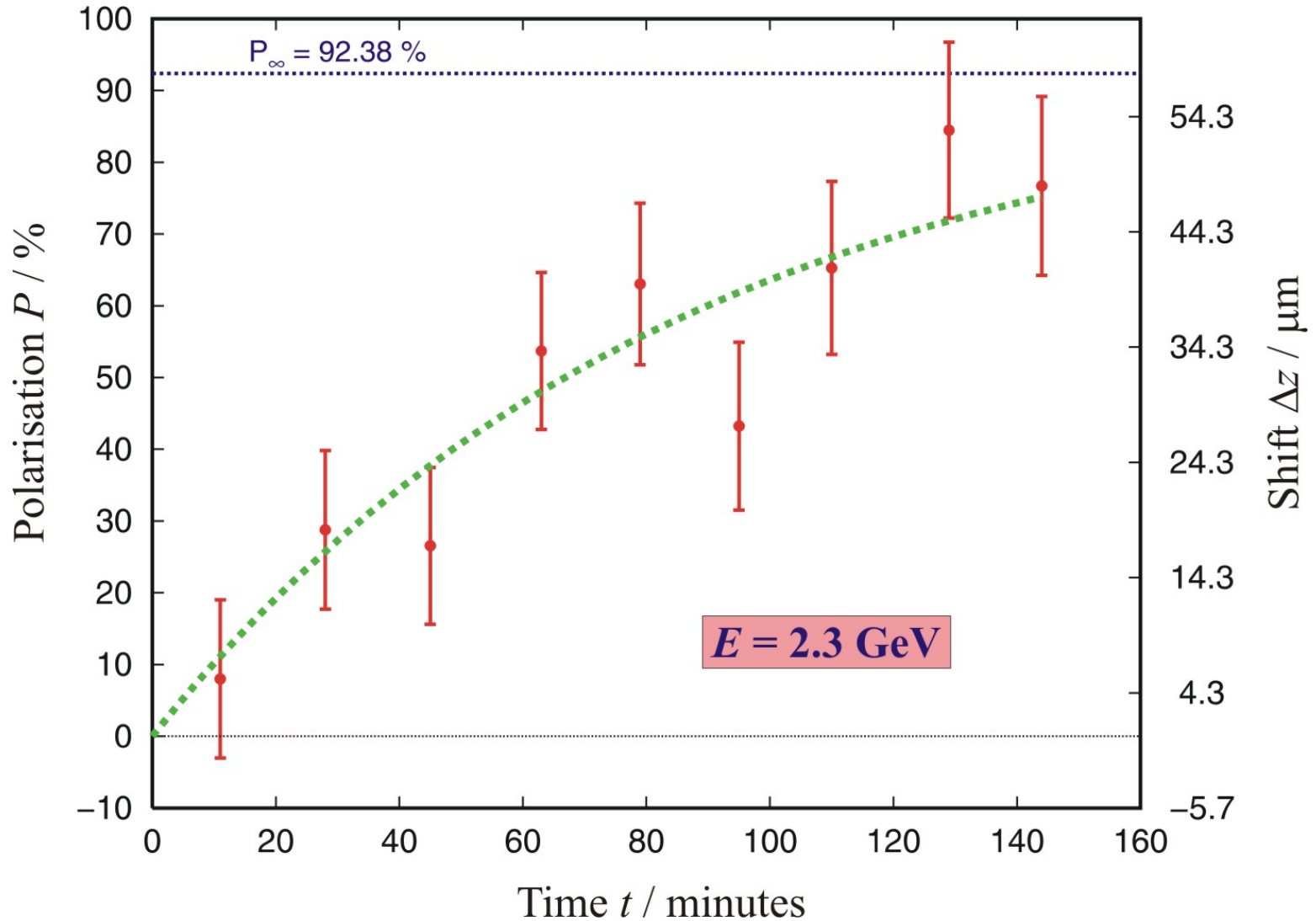
Signal / Background



Beam Profile



Sokolov-Ternov Mechanism



Problems:

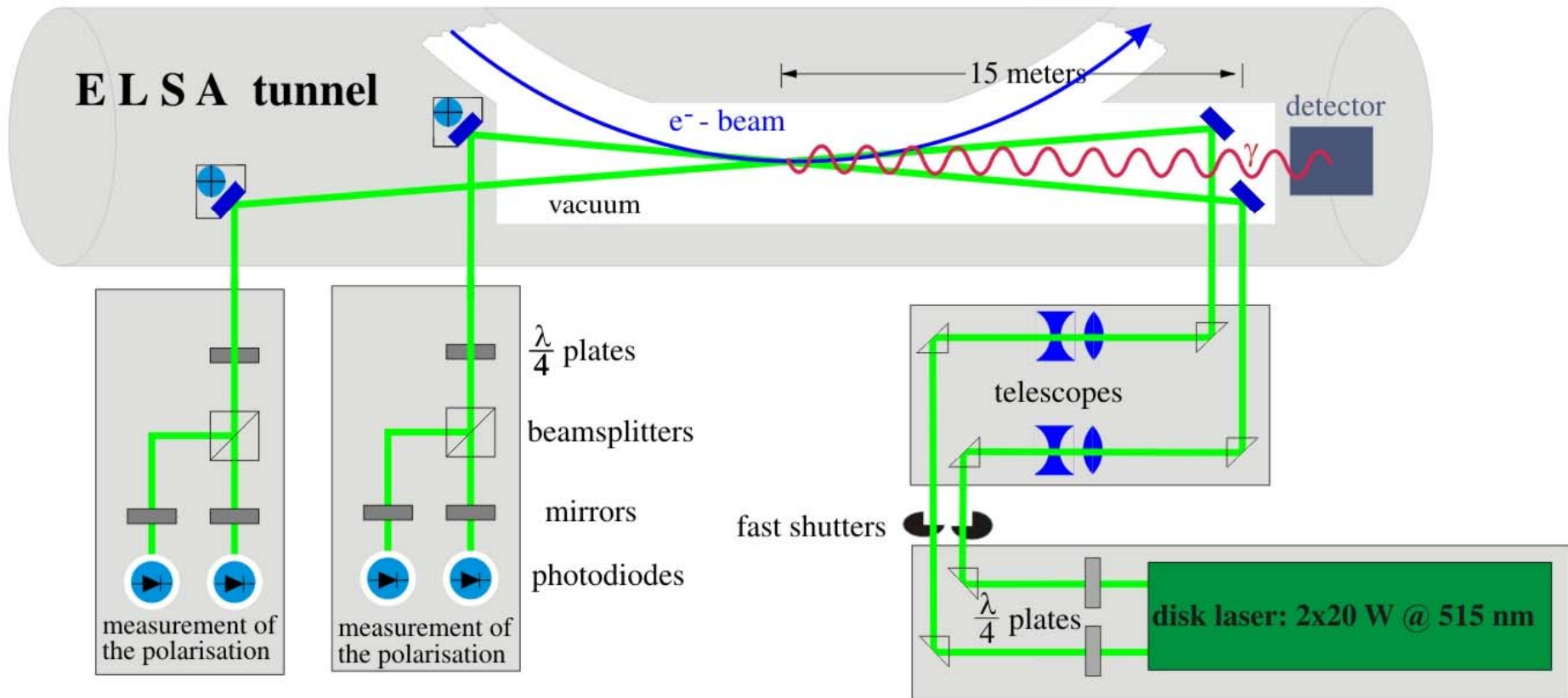
- **helicity correlated beam position** with feedback on
- high pressure at IP: $P > 10^{-7}$ mbar
- low laser power at IP: $P_L \approx 6.5$ W
- detector: **counter malfunctions**, $p = 100$ μm

➤ Improvements:

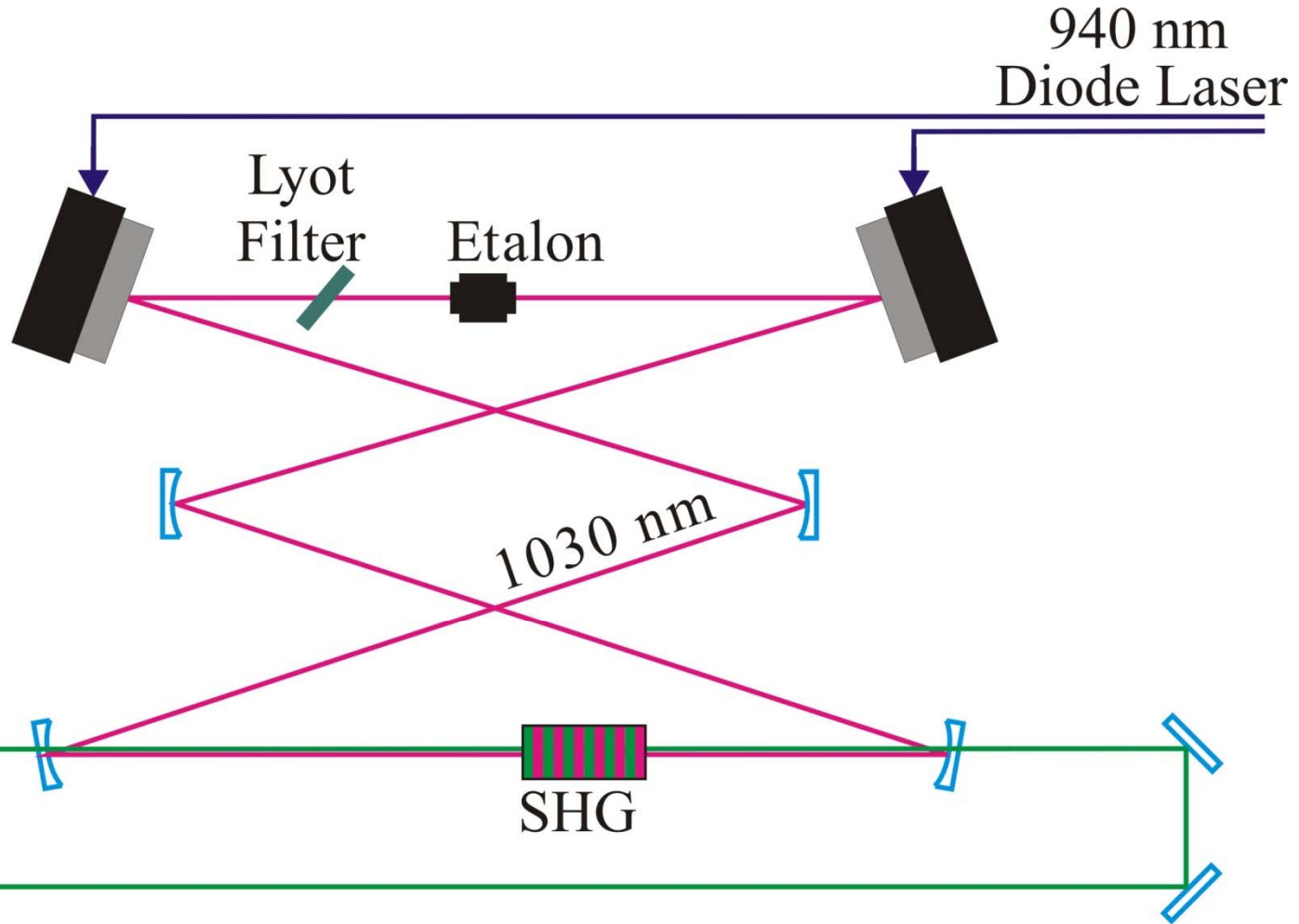
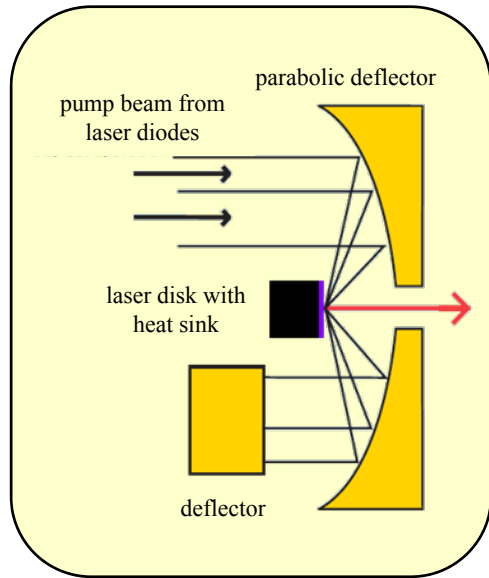
- additional IGP for IP: $P < 10^{-7}$ mbar
- new 2-beam disk-laser: $P_L > 40$ W
- **high beam pointing stability**, no feedback
- new detector electronics, LVDS: $p = 50$ μm

Future

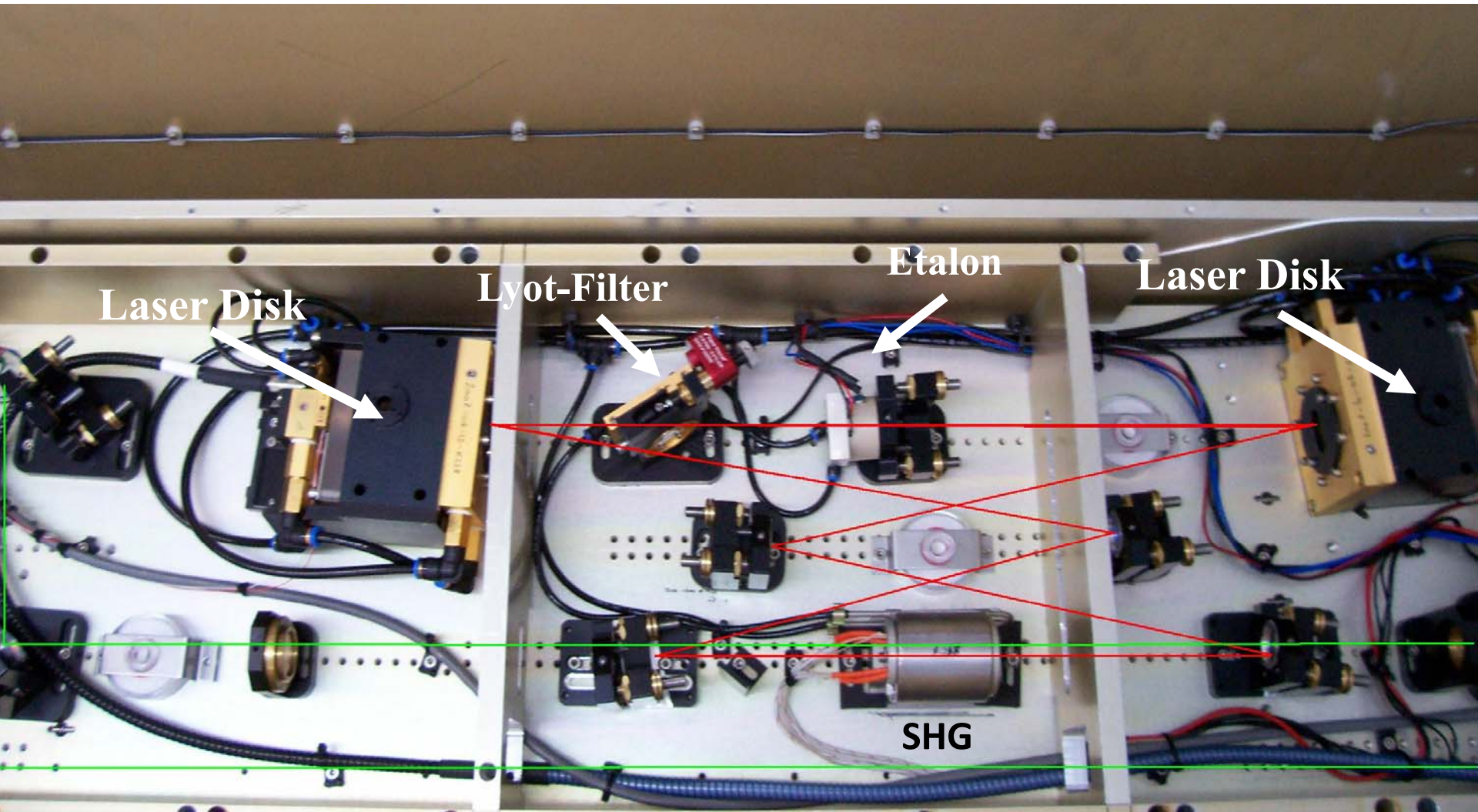
2-Beam Set-Up



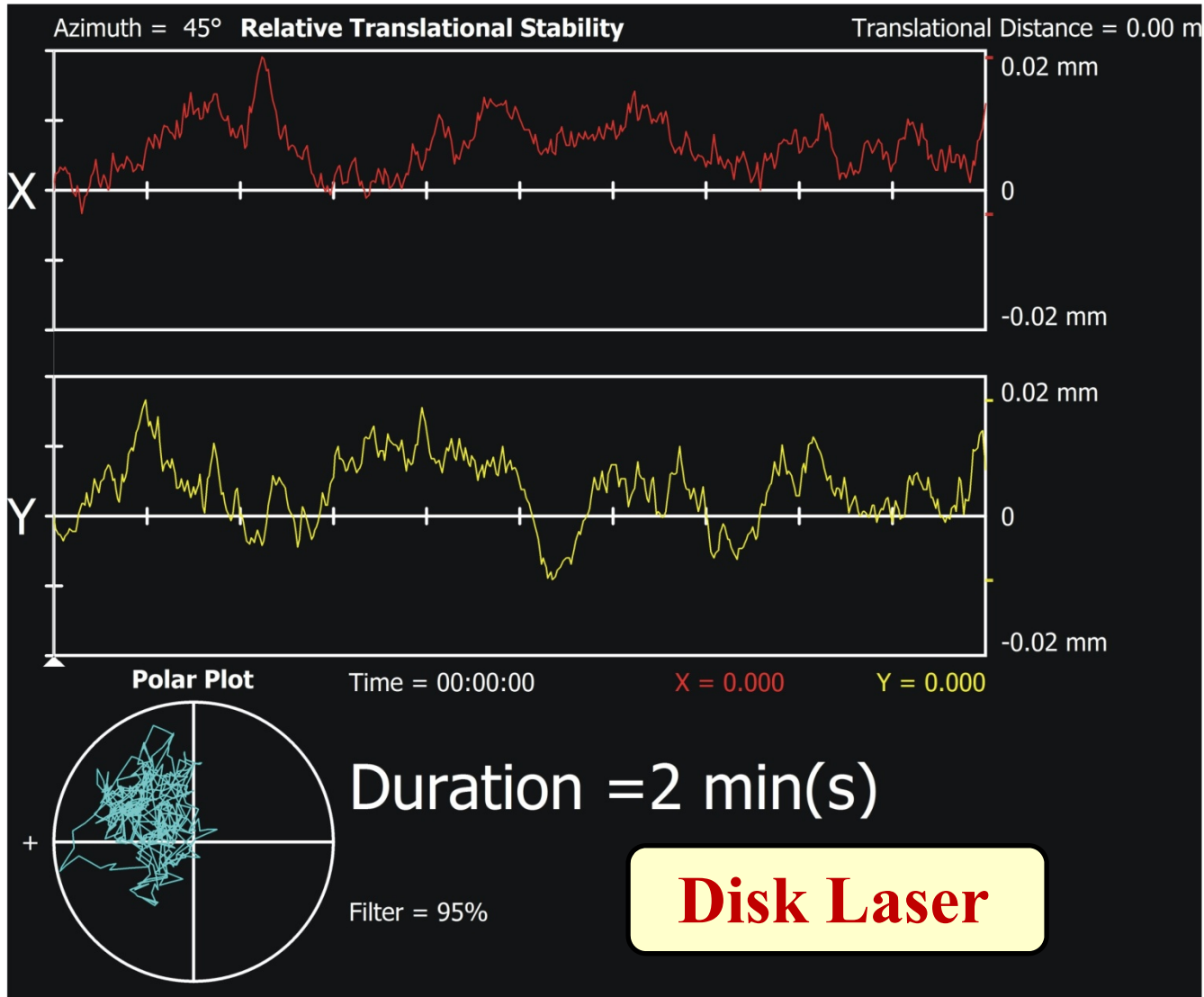
2 x 20 W Disk Laser



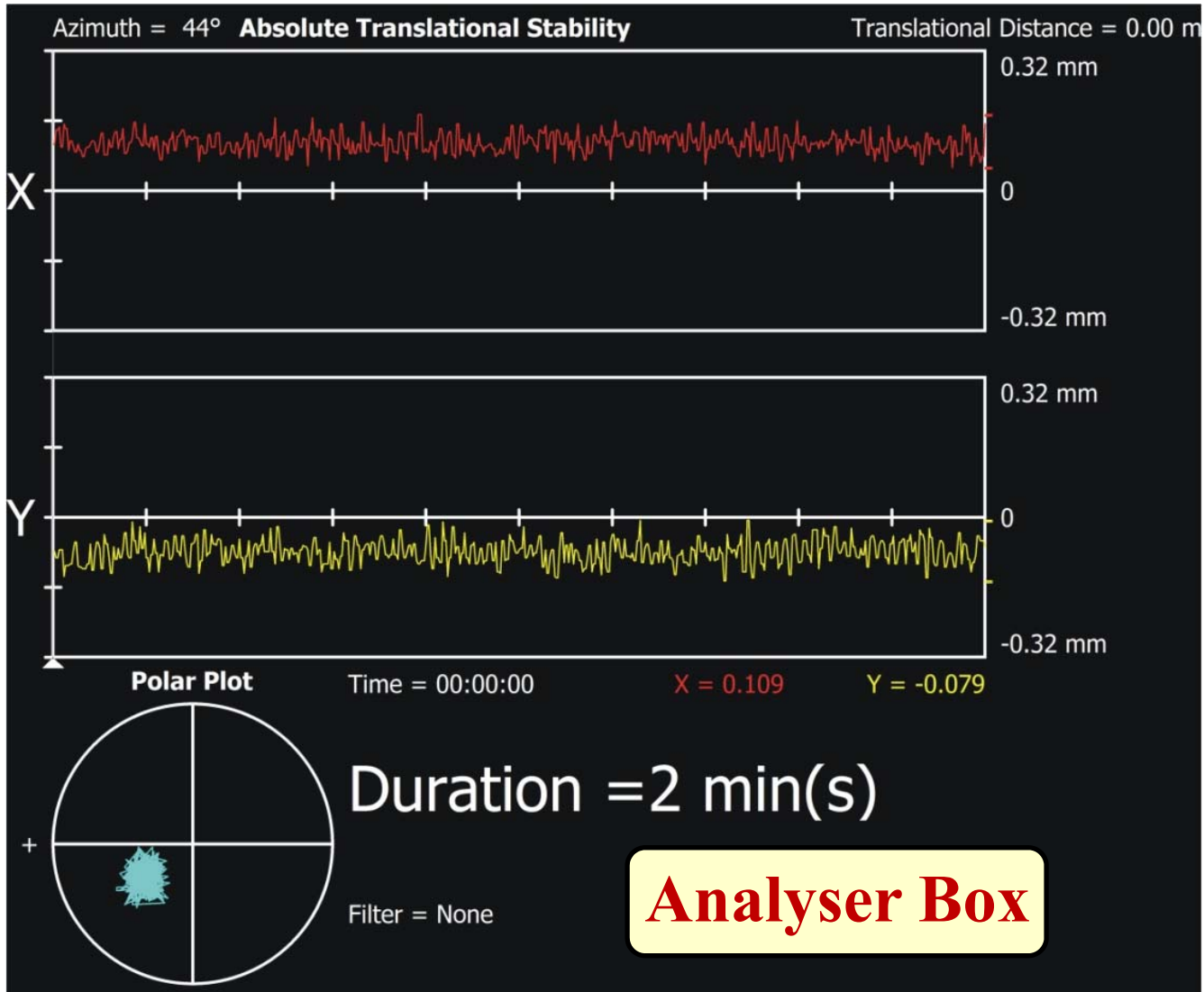
2 x 20 W Disk Laser



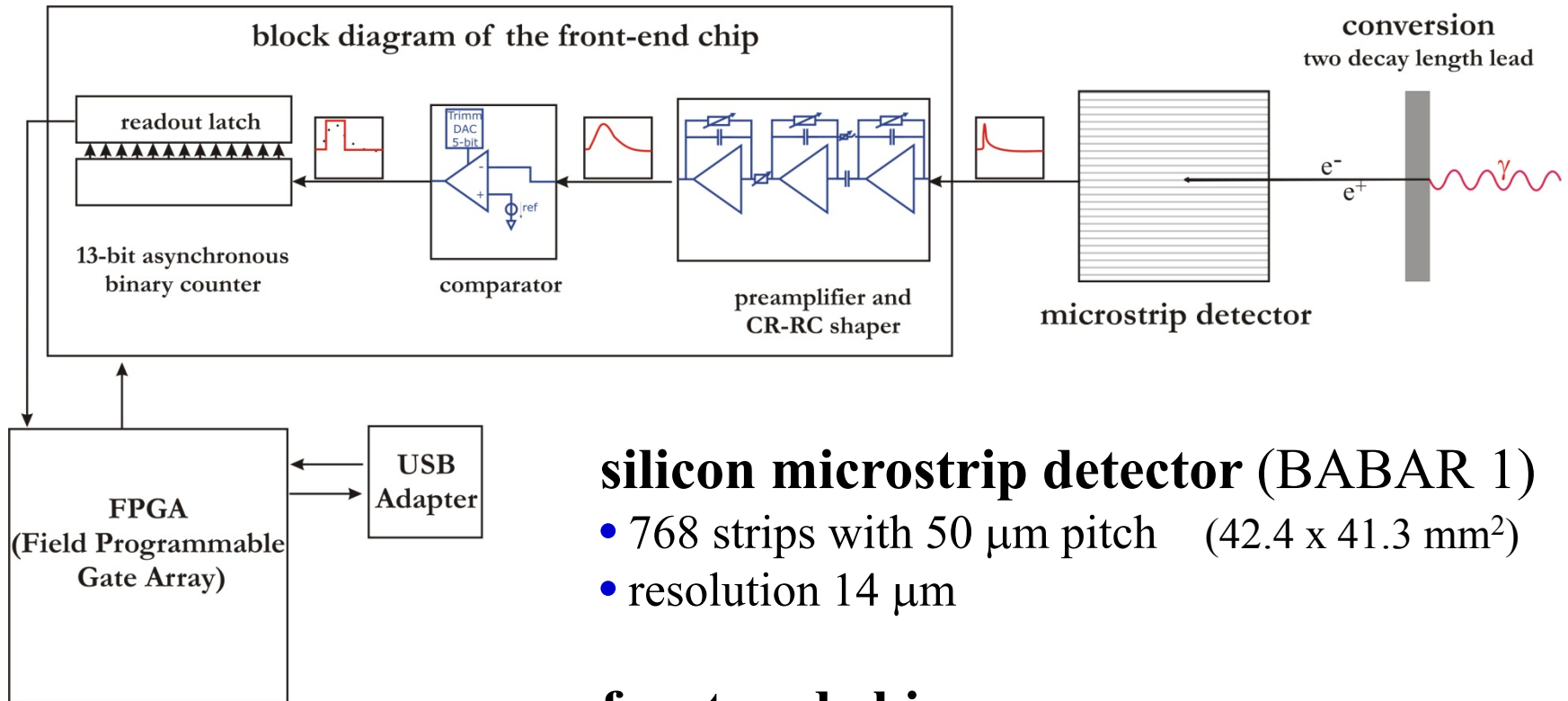
Beam Pointing Stability



Beam Pointing Stability



Detector Design



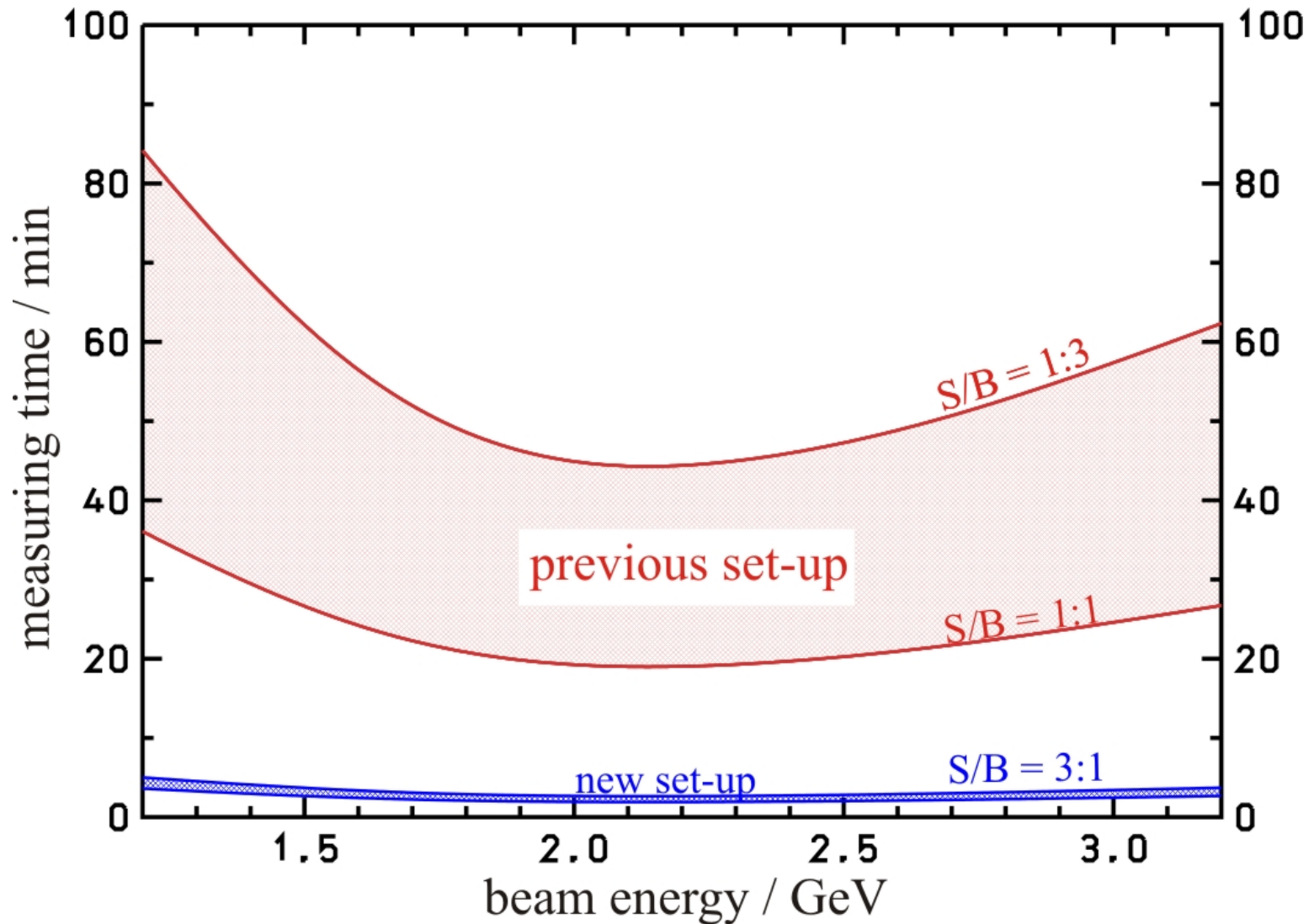
silicon microstrip detector (BABAR 1)

- 768 strips with $50 \mu\text{m}$ pitch ($42.4 \times 41.3 \text{ mm}^2$)
- resolution $14 \mu\text{m}$

front-end chip

- high rate acceptance (10 - 150 MHz)
- digital part built in LVDS technology
- FPGA controlled

Expected Measuring Time



Conclusions & Outlook



Polarimeter ready by 2009, enables:

- **precision polarimetry within minutes**
- **measurement of e^- – phase space in scanning mode**

Laser Optics

